ALIGNMENT-AWARE MODEL EXTRACTION ATTACKS ON LARGE LANGUAGE MODELS

Anonymous authors
Paper under double-blind review

ABSTRACT

Model extraction attacks (MEAs) on large language models (LLMs) have received increasing attention in recent research. However, existing attack methods typically adapt the extraction strategies originally developed for deep neural networks (DNNs). They neglect the underlying inconsistency between the training tasks of MEA and LLM alignment, leading to suboptimal attack performance. To tackle this issue, we propose Locality Reinforced Distillation (LoRD), a novel model extraction algorithm specifically designed for LLMs. In particular, LoRD employs a newly defined policy-gradient-style training task that utilizes the responses of victim model as the signal to guide the crafting of preference for the local model. Theoretical analyses demonstrate that I) The convergence procedure of LoRD in model extraction is consistent with the alignment procedure of LLMs, and II) LoRD can reduce query complexity while mitigating watermark protection through exploration-based stealing. Extensive experiments on domain-specific extractions validate the superiority of our method in extracting various state-of-the-art commercial LLMs. Our code is available at: https://anonymous.4open.science/r/LoRD-MEA-1EF2/.

1 INTRODUCTION

In recent years, we have witnessed the remarkable success of large language models (LLMs) such as ChatGPT cha (2024), Gemini Anil et al. (2024), and Claude cla (2024), which are now widely employed in various consumer and industrial applications. Despite their success, these models may suffer from *model extraction attacks* (MEAs) Krishna et al. (2020); Rafi et al. (2022); Xu et al. (2022); Li et al. (2023), where their knowledge could be at risk of being stolen by an adversary through a *local model* that learns on the data collected from the *victim model*. Besides of some "open-source" LLMs (e.g., Alpaca Taori et al. (2023)), which are trained on the chat history of GPT-4, cases of commercial model theft among companies have also been reported recently Heath (2023).

Under such a real-world threat, instead of focusing on MEAs against conventional DNNs, which have been extensively studied theoretically Saad & Solla (1995); Tian (2020); Zhou et al. (2021) and empirically Jagielski et al. (2020); Tramèr et al. (2016); Papernot et al. (2017), a few recent works turn to explore model

Figure 1: Comparison between vanilla MEAs on conventional DNNs (left) and MEAs on LLMs with alignments (right).

extraction algorithms and theorems for LLMs. For example, Wallace et al. (2020) propose a monolingual-query-based imitation attack framework to steal machine translation knowledge from generative language models such as GPT-2. Li et al. (2023) investigate threats of stealing the code-related knowledge from LLMs. However, these studies inherit those MEA algorithms from
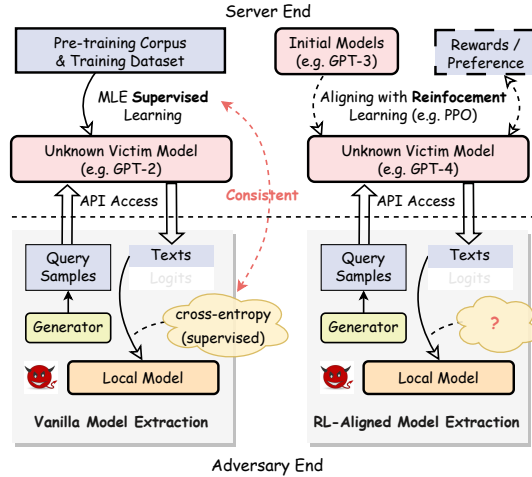
traditional fields, such as computer vision Tramèr et al. (2016); Papernot et al. (2017), and train the local model via supervised learning like maximum likelihood estimation (MLE) Bengio et al. (2000); Myung (2003), while neglecting the inconsistency of training tasks between MEAs and the alignments Ouyang et al. (2022); Glaese et al. (2022); Bai et al. (2022a;b); Perez et al. (2023) of modern LLMs. As shown in Figure 1, modern LLMs typically employ alignments using reinforced learning, which is missing in the local model training of conventional MEAs. As a result, these attacks usually suffer from poor performance.

In this paper, we challenge the effectiveness of MLE in stealing a reinforcement-learning-aligned LLM, by analyzing its potential drawbacks as follows:

Low query efficiency. Current LLM-oriented MEAs suffer from unacceptably significant query times because they must collect enough generated responses, which entails exponential complexity in terms of generated tokens, resulting in low query efficiency.

Vulnerability against defenses. Directly learning from the responses of victim models can cause local models to inadvertently incorporate those *watermarks* Cong et al. (2022); He et al. (2022); Zhao et al. (2022); He et al. (2021) embedded in the output of victim models. The residue of such watermarks makes the extraction process less stealthy and even serves as provenance evidence of model theft.

Motivated by these limitations, we propose <u>Lo</u>cality <u>R</u>ein-forced <u>D</u>istillation (LoRD), a query-efficient and watermark-resistant model extraction attack under a training paradigm with LLM's alignments. Stealing LLMs via reinforcement learning paradigms is challenging. The main reason is that the key component in the alignment procedure of LLMs, *reinforcement learning with human feedback* (RLHF) Bai et al. (2022a;b); Perez et al. (2023), heavily relies on the feedback signal of **human annotators**, which is difficult to reproduce directly in the context of MEAs. To tackle this challenge, we develop a policy-gradient-style extraction procedure. This approach regards the *locality direction* between the generations of local models and victim models as the implicit reward signal. It can thus achieve a **human-feedback-free** reinforcement learning for our extraction attack. From the theoretical perspective, we show why those existing MEAs using *MLE* and *knowledge distillation (KD)* are inconsistent with the optimization procedure in LLMs' alignments. Along this way, we also demonstrate why LoRD can achieve stronger watermark resistance and higher query efficiency.

Extensive experiments on five downstream NLP tasks and ten datasets demonstrate that it is feasible to steal a commercial LLM with 175 billion parameters by a pre-trained local model with only 8 billion parameters under a given domain. The resulting local model performs statistically similar to the victim model for tasks not requiring extra knowledge (e.g., data-to-text), and only $0 \sim 3$ percentage lower for tasks requiring it (e.g., translation and QAs). This result poses an immediate threat of task-specific extraction on commercial LLMs. To further draw the capability boundary of such a threat, we also illustrate the "spectrum" in difficulties and upper bounds for extracting LLMs.

To summarize, the contributions of our paper are as follows:

New Perspective of LLM Alignment for MEAs. We present LoRD, a novel model extraction attack algorithm for LLMs. To our best knowledge, it is the first effective and realistic extraction algorithm that is compatible with the alignment procedure of LLMs.

Theoretical Guarantee. We theoretically prove that the convergence procedure of LoRD in MEAs is consistent with the alignments of LLMs. Furthermore, we demonstrate that LoRD can reduce query complexity while mitigating watermark protection through exploration-based stealing.

Systematical Evaluation. Extensive experiments on domain-specific extractions demonstrate that our method outperforms current extraction strategies across different downstream NLP tasks.

2 BACKGROUND

2.1 POLICY GRADIENT MODELS

Policy gradient models (PGM) are commonly used in reinforcement learning (RL) algorithms to optimize the agents based on the decided *action* of RL agents. Represented by TRPO Schulman et al. (2015) and PPO Schulman et al. (2017), policy gradient models minimize the the following objective

function:

$$\mathcal{L}_{pg,j} = -\hat{\mathbb{E}}_j[p_j^r(\theta)A_j], \tag{1}$$

where at each decision step j, $p_j^r(\theta) = \frac{\pi_\theta(a_j|s_j)}{\pi_{\theta_{old}}(a_j|s_j)}$ refers to the probability ratio defined by the optimized policy $\pi_\theta(a_j|s_j)$ and the initial policy $\pi_{\theta_{old}}(a_j|s_j)$, s_j denotes the *state* of the environment, a_j denotes the decided *action* of π_θ, and A_j is the *de-biased reward* of a_j. A_j is estimated by the Q-value minus the V-value, i.e.,

$$A_j(s_j, a_j) = Q(s_j, a_j) - V(s_j). \tag{2}$$

Intuitively, Q-value refers to the *reward* if employing action a_j at the given environment state s_j, which can be seen as the label of policy's decision. V-value represents the estimation of the expected reward at s_j. Consequently, A_j denotes the *surprise* when taking action a_j.

To alleviate the *off the cliff* phenomenon that a large bad gradient update occurred from Equation 1, PGMs, such as PPO and TRPO, add some regularization terms to avoid large gradients. Specifically, TRPO constrains the distribution between π_θ and $\pi_{\theta_{old}}$ with KL divergence, and PPO warps a "clip" function to constrain the bounds of $p_j^r(\theta)$.

2.2 Language Modeling

Supervised Training (SFT). Given a pre-trained model with parameters θ, supervised training is essentially the *maximum likelihood estimation (MLE)* task Bengio et al. (2000); Myung (2003), which fine-tunes θ on the labeled dataset $\mathcal{D}_{tr}^s = \{(\mathbf{x}_i, \mathbf{y}_i)|i = 1, 2, ..., N_{trs}\}$ by minimizing the following objective function:

$$\mathcal{L}_{mle} = -\prod_i^{N_{trs}} P_\theta(\mathbf{y}_i|\mathbf{x}_i) = -\prod_i^{N_{trs}} \prod_j^N P_\theta(y_{i,j}|\mathbf{x}_i, \mathbf{y}_{i,<j}), \tag{3}$$

where N denotes the sequence length of $\mathbf{y}_i$, $y_{i,j}$ denotes the j-th token in $\mathbf{y}_i$, and $\mathbf{y}_{i,<j} = \{y_{i,0}, ..., y_{i,j-1}\}$. The logarithmic formula of Equation 3 can also be seen as a *joint cross-entropy* loss function:

$$\mathcal{L}_{ce} = -\sum_i^{N_{trs}} \log P_\theta(\mathbf{y}_i|\mathbf{x}_i) = -\sum_i^{N_{trs}} \sum_j^N \log P_\theta(y_{i,j}|\mathbf{x}_i, y_{i,<j}). \tag{4}$$

Equation 4 is extensively utilized in LLM's pre-training and fine-tuning procedures. For instance, it can be applied to *instruction-following supervised fine-tuning (SFT)* with the training set $\mathcal{D}_{tr}$, wherein $\mathbf{x}_i$ encompasses the instruction and the task input, while $\mathbf{y}_i$ denotes the reference response.

Aligning LLMs merely by SFT is not always practical, as MLE tends to align the model with the one-hot distribution of $\mathbf{y}$, making it challenging to draw a sufficient variety of examples due to the *"exponential explosion"* of tokens (see Section 4 for more details). Moreover, providing standard answers for LLMs can sometimes be daunting for annotators, which further slows down and even degrades the alignment process through direct training.

Therefore, instead of "learning from answers" as in Equation 4, learning from *preferences* is proposed, which only requires the annotators to select a better response from a pair of texts generated by LLMs.

Aligning from Preferences. Employing reinforcement learning in LLMs typically consists of three stages. First, the annotators construct a preference dataset $\mathcal{D}^{pref} = \{(\mathbf{x}_i, \mathbf{y}_i^+, \mathbf{y}_i^-)\}$ by chatting with LLMs and rating their responses, where $\mathbf{y}_i^+$ and $\mathbf{y}_i^-$ denote the rated positive and negative responses of the dialogue context $\mathbf{x}_i$, respectively. Then, a *reward model* $R_{\theta_\phi}(\mathbf{x}, \mathbf{y}) \to \mathbf{r}$ is trained based on $\mathcal{D}^{pref}$ to simulate the environment and predict the reward values of tokens in given texts. It is trained with a pair-wise loss,

$$\mathcal{L}_r = -\sum_{(\mathbf{x}, \mathbf{y}^+, \mathbf{y}^-) \sim \mathcal{D}^{pref}} \sigma(R_{\theta_\phi}(\mathbf{x}, \mathbf{y}^+) - R_{\theta_\phi}(\mathbf{x}, \mathbf{y}^-)), \tag{5}$$

where $\sigma(\cdot)$ denotes the sigmoid function. Based on the reward model $R_{\theta_\phi}(\mathbf{x}, \mathbf{y})$, we can finally train the language models P_θ by maximizing its reward, i.e.,

$$\max_\theta \sum_{\mathbf{x} \sim \mathcal{D}_q} R_{\theta_\phi}(\mathbf{x}, \hat{\mathbf{y}}) - \beta \mathbb{D}_{KL}[P_\theta(\mathbf{y}|\mathbf{x})||P_{\theta_{init}}(\mathbf{y}|\mathbf{x})], \tag{6}$$
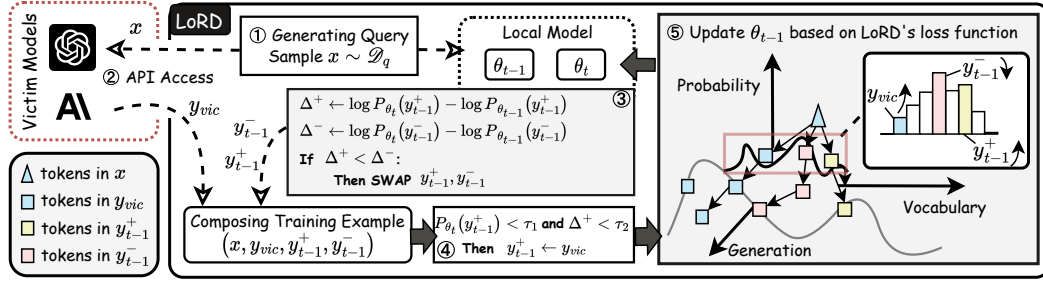
Figure 2: The stealing procedure of LoRD.

where $\mathcal{D}_q$ denotes the dataset of text inputs, $\hat{\mathbf{y}} \sim P_\theta(\mathbf{y}|\mathbf{x}))$ denotes the sampled sequence of the training model, and θ_{init} is the initialized parameters of the model, e.g. the parameters after SFT. The Kullback-Leibler (KL) divergence term, $\beta\mathbb{D}_{KL}[P_\theta(\mathbf{y}|\mathbf{x})||P_{\theta_{init}}(\mathbf{y}|\mathbf{x})]$, introduced by TRPO Schulman et al. (2015), is incorporated to constrain the shift of distribution in generated texts $\hat{\mathbf{y}}$, where β is the hyperparameter.

Consequently, SFT shown in Equation 4 fine-tunes the pre-trained model with parameters θ_{pre} into an aligned model θ_{sft} through MLE, and RLHF outlined in Equation 6, further aligns θ_{sft} towards the target model θ_{vic}. As this procedure is not consistent with the conventional training framework of DNNs, it remains unclear whether current MEAs (detailed in Appendix E.2) are effective and efficient in stealing a LLM. Specifically, we will first put forward a new stealing method in Section 3, and compare it with current MEAs in Section 4.

3 LoRD: LOCALITY REINFORCED DISTILLATION

3.1 OVERVIEW

In this subsection, we delve into the details of our model extraction framework, LoRD (Locality Reinforced Distillation). As described in Algorithm 1, LoRD follows a reinforcement learning paradigm, that is, it consists of several *periods*, and in each period, the model will learn to explore new responses and attempt to enhance the model trained in the last period. However, different from LLMs' alignments, the agent can neither obtain the reward from the reward model directly, nor label positive and negative responses manually. This motivates us to develop a locality-reinforced distillation method to address this issue.

Illustrated by Figure 2, the model samples two sentences randomly at period $t-1$, which are denoted as $\mathbf{y}_{t-1}^+$ and $\mathbf{y}_{t-1}^-$, respectively. In a new period t, we first compute the changes of
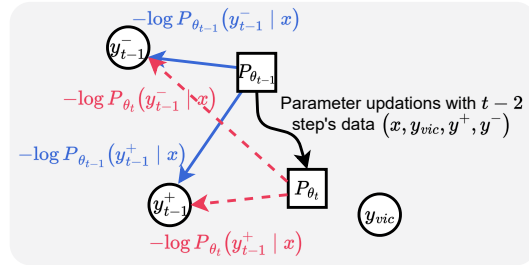

Figure 3: Determination of the positive and negative samples in LoRD. We sample $\mathbf{y}_{t-1}^+$ and $\mathbf{y}_{t-1}^-$ from $P_{\theta_{t-1}}(\cdot|\mathbf{x})$, and compute their conditional probabilities. The response with a higher probability increment on θ_t is selected as the positive sample.

likelihoods for these two sentences, among the old model $P_{\theta_{t-1}}$ and the current model P_{θ_t}. These changes of likelihoods, denoted as Δ_t^+ and Δ_t^-, indicate whether a selected sentence is locally *isotropic* ($\Delta > 0$) to the victim model's response $\mathbf{y}_{vic}$ or not ($\Delta \leq 0$), which can be seen as the feedback signal for P_{θ_t} in the current optimization step. For convenience, we may swap $\mathbf{y}_{t-1}^+$ with $\mathbf{y}_{t-1}^-$ to make sure that $\Delta_t^+ > \Delta_t^-$ always holds. In this way, for pairs $(\mathbf{x}, \mathbf{y}_{vic})$ we can take $\mathbf{y}_{t-1}^+$ as a *locality neighborhood* of $\mathbf{y}_{vic}$ and $\mathbf{y}_{t-1}^-$ as the negative sample, all of which can be utilized in the training of P_{θ_t}. Figure 3 illustrates this procedure. Additionally, we take $\mathbf{y}_{t-1}^+$ as the positive label under the current scope only when Δ^+ and $P_{\theta_t}(\mathbf{y}_{t-1}^+|\mathbf{x})$ both exceed their respective fixed thresholds

$\tau 1$ and τ_2. If these conditions are not met, we will use $\mathbf{y}_{vic}$ as a substitute for $\mathbf{y}_{t-1}^+$ to enable a cold start.

Based on $\mathbf{y}_{vic}$, $\mathbf{y}_{t-1}^+$, and $\mathbf{y}_{t-1}^-$, we now derive the loss function of LoRD.

3.2 DERIVATION OF LOSS FUNCTIONS

From Section 2.1, we know that the loss function of a policy gradient model can be expressed as an *objective function* to maximize the rewards of decisions (see Equation 1) and a *regularization term* to ensure the stability of training. Following this paradigm, the loss function of LoRD could be

$$\mathcal{L}_{\text{LoRD}} = \mathcal{L}_{obj} + \mathcal{L}_{reg}. \tag{7}$$

Objective function $\mathcal{L}_{obj}$. Following the definition of R_{θ_ϕ} in Equation 6, we use the logarithmic proportion between the positive sample and the negative sample as the de-biased reward, i.e., $\log P_{\theta_t}(\mathbf{y}_{t-1}^+|\mathbf{x}) - \log P_{\theta_t}(\mathbf{y}_{t-1}^-|\mathbf{x})$. Subsequently, we take $\log[P_{\theta_t}(\mathbf{y}_{vic}|\mathbf{x})/P_{\theta_{vic}}(\mathbf{y}_{vic}|\mathbf{x})]$, the proportion of the victim model to the local model, as the ratio term to scale such a reward.

Therefore, the objective function can be formatted as

$$\bar{\mathcal{L}}_{obj} = - \sum_{\mathbf{x} \in \mathcal{D}_q} |\log[\frac{P_{\theta_{vic}}(\mathbf{y}_{vic}|\mathbf{x})}{P_{\theta_t}(\mathbf{y}_{vic}|\mathbf{x})}]| \cdot \log[\frac{P_{\theta_t}(\mathbf{y}_{t-1}^+|\mathbf{x})}{P_{\theta_t}(\mathbf{y}_{t-1}^-|\mathbf{x})}] = - \sum_{\mathbf{x} \in \mathcal{D}_q} [\frac{\log P_{\theta_t}(\mathbf{y}_{t-1}^+|\mathbf{x}) - \log P_{\theta_t}(\mathbf{y}_{t-1}^-|\mathbf{x})}{|\log P_{\theta_t}(\mathbf{y}_{vic}|\mathbf{x}) - \log P_{\theta_{vic}}(\mathbf{y}_{vic}|\mathbf{x})|}],$$

where $|\cdot|$ indicates no gradient back propagation, t and $\mathbf{x} \sim \mathcal{D}_q$ denote the training period and the sampled query text, respectively. Since it is impractical to obtain the victim model's probability $P_{\theta_{vic}}(\mathbf{y}_{vic}|\mathbf{x})$ under black-box settings, we simplify $\bar{\mathcal{L}}_{obj}$ by setting $P_{\theta_{vic}}(\mathbf{y}_{vic}|\mathbf{x}) = 1$, and remove $P_{\theta_t}(\mathbf{y}_{vic}|\mathbf{x})$ to ensure the stability in the black-box extraction, i.e.,

$$\mathcal{L}_{obj} = - \sum_{\mathbf{x} \in \mathcal{D}_q} \log[\frac{P_{\theta_t}(\mathbf{y}_{t-1}^+|\mathbf{x})}{P_{\theta_t}(\mathbf{y}_{t-1}^-|\mathbf{x})}] = - \sum_{\mathbf{x} \in \mathcal{D}_q} [\log P_{\theta_t}(\mathbf{y}_{t-1}^+|\mathbf{x}) - \log P_{\theta_t}(\mathbf{y}_{t-1}^-|\mathbf{x})]. \tag{8}$$

Regularization loss $\mathcal{L}_{reg}$. Current studies Schulman et al. (2015); Rafailov et al. (2023); Bai et al. (2022a) tend to constrain θ_t with initial model's generating distribution $P_{\theta_{init}}(\cdot|\mathbf{x})$ in RLHF. However, this strategy requires re-loading an extra initial model's weights, which is memory-consuming. Also, the KL-divergence term $\mathbb{D}_{KL}(P_{\theta_t}||P_{\theta_{init}})$ consists of $P_{\theta_t}(\cdot|\mathbf{x})$, which requires an extra exponential operation of $\log P_{\theta_t}(\cdot|\mathbf{x})$ that will slow down the forward computation procedure.[1] Therefore, in MEAs, we put forward a regularization based on the victim model, where only the logarithmic part of KL divergence is employed and only the dimension of selected tokens is used in KL divergence, i.e.,

$$\mathcal{L}_{reg} = - \sum_{\mathbf{x} \in \mathcal{D}_q} clip(\log[\frac{P_{\theta_t}(\mathbf{y}_{vic}|\mathbf{x})}{P_{\theta_t}(\mathbf{y}_{t-1}^-|\mathbf{x})}]) = - \sum_{\mathbf{x} \in \mathcal{D}_q} clip(\log P_{\theta_t}(\mathbf{y}_{vic}|\mathbf{x}) - \log P_{\theta_t}(\mathbf{y}_{t-1}^-|\mathbf{x})). \tag{9}$$

In Equation 9, we utilize a $clip(\cdot)$ function to limit the value of the regularization term, as we expect the regularization term could only be used to avoid the *off the cliff* problem Schulman et al. (2017; 2015) in RL's convergence and the *shift of the distribution* Rafailov et al. (2023) in LLMs' alignments.

Incorporating Equation 8 with Equation 9, we can reshape the loss function of LoRD as

$$\mathcal{L}_{\text{LoRD}} = \mathcal{L}_{obj} + \mathcal{L}_{reg} = \sum_{\mathbf{x} \in \mathcal{D}_q} \log[\frac{P_{\theta_t}(\mathbf{y}_{t-1}^-|\mathbf{x})}{P_{\theta_t}(\mathbf{y}_{t-1}^+|\mathbf{x})}] + clip(\log[\frac{P_{\theta_t}(\mathbf{y}_{t-1}^-|\mathbf{x})}{P_{\theta_t}(\mathbf{y}_{\text{vic}}|\mathbf{x})}])]. \tag{10}$$

Finally, we wrap $\mathcal{L}_{\text{LoRD}}$ with a sigmoid function $\sigma(\cdot)$ to normalize the loss to the interval $(0,1)$, which is

$$\mathcal{L} = \sum_{\mathbf{x} \sim \mathcal{D}_q} \sigma(\log[\frac{P_{\theta_t}(\mathbf{y}_{t-1}^-|\mathbf{x})}{P_{\theta_t}(\mathbf{y}_{t-1}^+|\mathbf{x})}] + clip(\log[\frac{P_{\theta_t}(\mathbf{y}_{t-1}^-|\mathbf{x})}{P_{\theta_t}(\mathbf{y}_{vic}|\mathbf{x})}])). \tag{11}$$

---

[1] *logsoftmax* is preferred in the implementation of deep learning frameworks tor, as the exponential operation in *softmax* and the logarithmic operation in *cross-entropy* can be canceled out by each other.

4 THEORETICAL ANALYSIS

This section will compare LoRD with current model extraction methods from a theoretical perspective. We will first reveal the underlying inconsistency between the optimization procedure of LLMs, which typically involves RL-based alignments, and the previous model extraction approaches utilizing *MLE* and *knowledge distillation (KD)*. Subsequently, we will demonstrate in theory the reasons why LoRD can achieve stronger watermark resistance and higher query efficiency than existing methods.

4.1 CONSISTENCY ANALYSIS REGARDING DIFFERENT LEARNING TASKS

Based on the analysis of the four objective functions for MLE, KD, RLHF and LoRD, we reach the proposition 1, and illustrate their convergence procedure exhibited in Figure 4. A detailed proof can be found in Appendix D.1.

Proposition 1 (Consistency in Stealing Procedure). *The learning procedure for LLMs' alignments is consistent with the stealing procedure of LoRD, i.e., they both attempt to maximize the difference between the probabilities of positive and negative samples. Conversely, they are inconsistent with either MLE or KD. In MLE, the objective is maximizing the label probability, while KD aims to minimize the distance among all dimensions.*

Albeit the inconsistency in their *training procedures*, we put forward Proposition 2 to demonstrate that *with enough samples*, all these methods will reach the same distribution results.

Proposition 2 (Equivalence when Converged). *Ideally, for any loss value of Equations 4, 5, 6, 10, or 11 converging to* 0, *we have* $\mathbf{y}^+ \equiv \mathbf{y}_{vic}$. *Meanwhile, the local model's distribution* $P_\theta(\cdot|\mathbf{x})$ *will approach that of the victim model* $P_{\theta_{vic}}(\cdot|\mathbf{x})$ *on MEAs from all three discussed MEA methods, including LoRD, MLE, and KD.*

Proposition 2 ensures that the local model will converge to the victim model **regardless** of the choice of MEA methods. So what is the benefit of LoRD? In Section 4.2, we will show that LoRD outperforms current MEAs with two aspects: the query time reduction (i.e., size of the query set $\mathcal{D}_q$), and the watermark resistance of the learned local model.
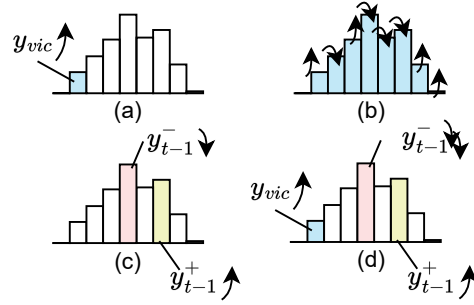

Figure 4: Illustrations for the converging procedure of probability distributions regarding four methods, namely MLE (a), KD (b), RLHF (c), and LoRD (d). Arrows indicate the expected optimization direction. We mark the distribution dimensions learned with labels in *blue*, and employ *pink* and *yellow* components to indicate the probabilities of positive and negative tokens, respectively.

4.2 COMPARATIVE ANALYSIS ON MODEL STEALING

Query Efficiency. Let N_Q and N_R denote the sequence lengths of the query text and the response text, respectively. For MLE, the *ideal* query numbers to populate the entire text space are given by $\mathcal{O}(V^{N_Q} \cdot V^{N_R})$, where V represents the size of the vocabulary. In contrast, the ideal query times for LoRD can be reduced to $\mathcal{O}(V^{N_Q} \cdot C)$, with C being a constant. This constant suggests that the model requires only a fixed and limited number per query, as LoRD itself can automatically generate and explore V^{N_R} possibilities during training.

Based on the above analysis, a straightforward concern with employing MLE in LLMs' extraction is that, given the limited query times in real-world practices, it may suffer from incomplete learning, especially for text generation tasks. Consequently, the local model may tend to memorize some specific responses instead of achieving a broad understanding and generation. We call such a phenomenon *preference overfitting (PO)*, which indicates that the local model is only effective on a limited set of explored samples, and yet does not generalize well to unseen scenarios. In such cases, the local model usually exhibits a more "rugged" decision surface, which appears to *overfit* the preference sentences in $\mathcal{D}_{tr}$, as shown in Figure 11 (b). Figure 10 provides a visualization of it.

	BLEU				BERTScore			Rouge-L		
	1	2	3	4	Pre.	Rec.	F1.	Pre.	Rec.	F1.
Text to SQL: WikiSQL Zhong et al. (2017) with 64 query samples										
Victim Model	54.1	41.4	32.1	24.4	86.9	93.5	90.1	58.9	62.1	59.7
Local Model	20.2±0.2	14.5±0.2	10.9±0.1	8.1±0.1	82.5±0.0	92.4±0.1	87.1±0.0	22.6±0.3	66.4±0.4	33.2±0.3
+MLE	54.0±1.6	37.5±2.1	26.4±2.0	18.8±1.8	83.1±0.2	92.9±0.2	87.7±0.2	56.2±1.5	56.1±0.9	55.8±1.2
+LoRD	55.1±2.3	39.0±3.6	28.0±4.0	20.4±3.9	83.4±0.4	92.9±0.3	87.9±0.4	57.7±2.2	56.3±2.0	56.7±2.1
Text to SQL: Spider Zhong et al. (2017) with 64 query samples										
Victim Model	9.4	3.9	2.1	1.1	77.7	84.1	80.6	17.1	36.3	21.8
Local Model	6.4±0.2	2.1±0.1	0.9±0.1	0.5±0.0	80.0±0.1	82.6±0.1	81.2±0.1	10.0±0.3	21.5±0.6	12.7±0.4
+MLE	6.2±0.9	1.3±0.5	0.6±0.3	0.2±0.0	76.4±0.7	81.8±0.4	78.9±0.6	12.7±1.6	18.3±1.6	14.3±1.6
+LoRD	9.1±0.9	2.8±0.5	1.3±0.4	0.6±0.2	77.7±0.4	83.1±0.5	80.2±0.3	16.9±0.1	24.1±0.2	18.8±0.1
Data to Text: E2E NLG Dušek et al. (2020) with 64 query samples										
Victim Model	51.8	27.0	26.8	19.1	93.9	94.6	94.2	49.6	54.6	51.4
Local Model	31.1±0.1	20.1±0.2	13.5±0.2	8.9±0.3	86.1±0.1	92.4±0.1	89.1±0.1	29.0±0.3	49.4±0.4	35.9±0.3
+MLE	53.0±0.9	38.0±0.6	27.5±0.5	19.9±0.4	89.1±0.0	94.5±0.0	91.8±0.0	48.3±0.5	54.2±1.4	50.4±0.9
+LoRD	53.1±1.1	38.2±0.9	27.8±0.7	20.2±0.5	89.1±0.1	94.5±0.1	91.7±0.1	48.3±0.7	53.5±1.4	50.2±0.9
Data to Text: CommonGen Lin et al. (2020) with 64 query samples										
Victim Model	33.3	18.5	11.1	6.9	91.3	92.1	91.7	33.6	40.7	36.1
Local Model	12.2±0.0	6.5±0.1	3.8±0.0	2.3±0.0	83.0±0.0	89.7±0.0	86.2±0.0	14.6±0.1	46.2±0.2	21.6±0.0
+MLE	32.4±2.0	18.3±1.3	10.9±1.0	6.6±0.7	84.2±0.1	91.7±0.0	87.8±0.0	31.7±2.4	41.1±0.4	35.1±1.6
+LoRD	32.1±1.3	18.0±0.9	10.7±0.5	6.4±0.3	84.1±0.0	91.6±0.1	87.7±0.0	31.4±1.1	40.3±0.9	34.6±0.9
Summarization: TLDR Kirk et al. (2023) with 64 query samples										
Victim Model	11.9	5.0	2.6	1.5	85.9	88.4	87.1	13.4	30.9	18.4
Local Model	6.9±0.0	3.2±0.1	1.7±0.0	1.0±0.0	81.0±0.1	87.6±0.0	84.1±0.0	10.5±0.1	41.1±0.1	16.4±0.1
+MLE	10.6±0.5	4.8±0.2	2.6±0.1	1.6±1.1	83.6±0.7	88.4±0.2	85.9±0.5	14.3±0.5	32.7±1.1	18.9±0.4
+LoRD	10.2±0.3	4.5±0.1	2.4±0.1	1.4±0.0	84.0±0.1	88.3±0.1	86.2±0.1	12.8±0.3	33.2±0.9	18.0±0.2
Summarization: CNN Daily Mail Hermann et al. (2015) with 64 query samples										
Victim Model	20.4	10.8	6.4	4.1	86.4	87.8	87.1	22.4	40.8	28.2
Local Model	4.9±0.0	3.6±0.0	2.7±0.0	2.1±0.0	80.5±0.0	88.3±0.0	84.2±0.0	10.9±0.0	79.1±0.1	18.8±0.0
+MLE	5.1±0.5	3.7±0.0	2.8±0.0	2.2±0.0	80.6±0.0	88.3±0.0	84.3±0.0	11.3±0.1	78.6±0.1	19.3±0.1
+LoRD	5.3±0.0	3.9±0.0	2.9±0.0	2.3±0.0	80.6±0.0	88.4±0.0	84.3±0.0	11.3±0.1	78.6±0.2	19.1±0.1
Summarization: Samsum Gliwa et al. (2019) with 64 query samples										
Victim Model	20.7	11.4	6.9	4.4	88.1	91.7	89.8	24.2	50.5	31.6
Local Model	8.9±0.2	5.2±0.1	3.3±0.1	2.1±0.1	80.9±0.2	90.1±0.1	85.2±0.2	17.0±0.3	61.8±0.5	25.5±0.4
+MLE	16.9±1.1	9.4±0.7	5.8±0.4	3.7±0.3	83.9±0.9	90.9±0.6	87.3±0.8	25.2±0.8	49.8±2.5	31.0±1.7
+LoRD	18.4±0.7	10.1±0.3	6.0±0.2	3.7±0.1	84.9±0.1	91.5±0.1	88.1±0.1	23.2±0.8	49.7±1.5	30.2±0.6

Table 1: MEA comparison on three tasks, including structured text generation, data to text, and summarization. We use GPT-3.5-turbo as the victim model, and Llama3-8B lla (2024) as the local initial model. The *intensity* of the red or blue color corresponds to the degree of underperformance or outperformance relative to the victim model. More experiments are in Table 2 and Table 5.

Watermark Resistance. Another limitation of prevalent objective functions, such as MLE and KD, is their susceptibility to watermarks Cong et al. (2022); He et al. (2022; 2021); Kirchenbauer et al. (2023) of output contents, i.e., while stealing knowledge from LLMs via responses $\mathbf{y}_{vic}$, watermarks within them will also been passively inherited by the local model. Consequently, the generated sentences of the local model may possess some *residual* of watermarks, which might be detected as evidence of stealing.

Despite introducing current watermark removal techniques, we indicate that LoRD can mitigate the influences of watermarks naturally, as it does not learn the likelihood of victim models' responses $\mathbf{y}_{vic} \sim \mathcal{D}_{tr}$ directly, but relies on $\mathbf{y}_{vic}$ to determine positive and negative labels from responses generated by the local model.

As depicted in Equation 8, LoRD guides the local model to learn the likelihood of $\mathbf{y}_{t-1}^{+}$ instead of $\mathbf{y}_{vic}$, which means that it will not been influenced by watermarks contained in $\mathbf{y}_{vic}$ explicitly. However, the regularization term $\mathcal{L}_{reg}$, as well as the replacement $\mathbf{y}_{t-1}^{+} \leftarrow \mathbf{y}_{vic}$ for a cold start, will indeed introduce watermarks from $\mathbf{y}_{vic}$. To address this, we can reshape Equation 11 into a convex combination of the objective function and the regularization, i.e.,

$$\mathcal{L} = \mathbb{E}[(1-\lambda_1) \cdot (\log P_{\theta_t}(\mathbf{y}_{t-1}^{+}|\mathbf{x}) - \log P_{\theta_t}(\mathbf{y}_{t-1}^{-}|\mathbf{x})) + \lambda_1 \cdot clip(\log P_{\theta_t}(\mathbf{y}_{vic}|\mathbf{x}) - \log P_{\theta_t}(\mathbf{y}_{t-1}^{-}|\mathbf{x}))],$$

where $0 \leq \lambda_1 \leq 1$ is the hyperparameter.

When λ_1 is small, the convergence of LoRD will substantially focus on maximizing $P_{\theta_t}(\mathbf{y}_{t-1}^{+}|\mathbf{x})/P_{\theta_t}(\mathbf{y}_{t-1}^{-}|\mathbf{x})$, with which the local model will exhibit a strong watermark resistance ability. When λ_1 increases, LoRD will tend to rely more on the guidance of $\mathbf{y}_{vic}$, resulting in a higher risk of introducing watermarks. In the case of $\lambda_1 = 1$, the local model will converge to the victim model without any exploration and watermark resistance, which might suffer from the same level of defense by watermarks.

From a global perspective, $\mathcal{L}_{obj}$ represents the exploration and the locality learning ability of LoRD, which can mitigate the influences of watermarks. On the other hand, $\mathcal{L}_{reg}$ ensures the stability of

the training procedure. Therefore, $\mathcal{L}$ characterizes a trade-off via λ_1 between the stability and the diversity during stealing, and Equation 11 can be seen as a special case of $\mathcal{L}$ with $\lambda_1 = 0.5$.

5 EXPERIMENTS

5.1 SETTINGS

Datasets. We evaluate MEAs on five mainstream natural language generation (NLG) tasks, including *machine translation*, *text summarization*, *question answering*, *structured text generation*, and *data-to-text*. We select ten representative datasets: WMT16 Bojar et al. (2016), TLDR Kirk et al. (2023), CNN Daily Mail Hermann et al. (2015), Samsum Gliwa et al. (2019), WikiSQL Zhong et al. (2017), Spider Yu et al. (2018), E2E-NLG Dušek et al. (2020), CommonGen Lin et al. (2020), PIQA Bisk et al. (2020), and TruthfulQA Lin et al. (2021) as benchmarks for our domain-specific evaluation. These datasets cover most of the downstream tasks in natural language generation. We compare not only the stealing efficacy of different MEA methods, but also the stealing difficulty across different downstream tasks. Table 4 lists all datasets and backbones used in the paper.

Baselines. As described in Section 2.2 and 4.1, we compare LoRD with two types of model extraction methods: maximum likelihood estimation (MLE) and knowledge distillation (KD). For MLE and LoRD, we conduct MEAs under pure **black-box attack settings** (see Appendix F for more details of the threat model). For KD, the predicted distributions are used specifically under grey-box settings.

Metrics. For text generation tasks, we evaluate extracted models with a semantic-level and two lexical-level metrics, BERTScore Zhang et al. (2020), BLEU Papineni et al. (2002), and Rouge-L Lin (2004), all of which are commonly used in the NLG evaluation. Regarding reasoning tasks (e.g., QA), we use Precision, Recall, Accuracy, and F1 score as their evaluation metrics.

Implementation Details. We use Llama3-8B as the local model to learn the outputs generated by victim models. We set sequence length varying 128 to 4096 depending on the selected tasks, and learning rate 3×10^{-5}. Our experiments run on 2×80GB Nvidia Tesla A100. We execute each training five times and record the mean values and standard variances in the following sections. For LoRD, we set τ_1 and τ_2 to 0.8 and -0.1, respectively. Besides, we set the period number N_t to 512, and use $\lambda_1 = 0.5$ as the default formation of the loss function. The victim model's response, $\mathbf{y}_{vic}$, is generated by token sampling with a temperature of 1, the default setting for current LLM APIs. The local model also uses token sampling, but with a temperature of 0.8 and Top-P probability clipping Holtzman et al. (2019) at 0.98. We use this setting to enhance the stability of generation in local models. Note that we have not incorporated *sampling strategies* with their corresponding hyperparameters into the design of LoRD. We believe that MEAs considering sampling strategies could inspire more powerful MEA methods, and we leave these improvements for future work.

5.2 STEALING DOMAIN-SPECIFIC KNOWLEDGE

We first select GPT-3.5-turbo, a checkpoint of ChatGPT, as the basic victim model. This is because its API provides *probabilities* of candidate words when generating responses. We employ Llama3-8B lla (2024), a small LLM with only a 4.5% fraction of parameters than the victim model as our initial local model. Though this LaViSH (**La**rge-**Vi**ctim-**S**mall-**H**eist) setting contradicts previous assumptions Tramèr et al. (2016); Papernot et al. (2017); Jagielski et al. (2020) in MEA that the copy model should usually be "wider" or "larger" than the victim model to contain its knowledge, we believe this setting is more applicable in real world scenarios Li et al. (2023). Appendix F provides more detail for this setting. Besides, the number of query times selected in this section is less than 100, a significant degradation compared to previous studies Li et al. (2023). This is because, in our experiments, copy models can easily learn the knowledge with a few training samples and then exhibit only slight improvements afterward. More discussions on query times can be found in Appendix C.1.1.

Fidelity and limits on stealing. We first examine the fidelity and limits of a small LLM to steal commercial LLMs. As shown in Table 1, we list the performance of the victim model and the local model on three tasks, and provide two MEA methods, local model fine-tuned with MLE (+MLE) and LoRD (+LoRD), respectively. In Table 1, cells highlighted in *red* indicate poorer outcomes compared to the victim model, whereas *blue* signifies results that are on par or potentially superior to the victim

model. The *intensity* of the red or blue color corresponds to the degree of underperformance or outperformance relative to the victim model.

We can see that the original performance of the local model is significantly lower than the victim model, i.e., with a 50% decrease in BLEU-4 or $10 \sim 25$ decrease in Rouge-L. Once we employ MEAs in the local model, its performance rapidly boosts to nearly the same as the victim model, with $0 \sim 40\%$ points of gaps in BERTScore. These gaps are negligible (e.g. $< 1\%$ in summarization) in some tasks, but remain eminent in other tasks such as reasoning, structured text generation, and machine translation. This phenomenon indicates that domain-specific model extractions can effectively learn domain-specific abilities from victim models but may perform poorly if downstream tasks require extra knowledge, such as machine translation and QA.

Comparison among stealing methods. Tables 1, 5, and 2 compare the stealing efficacy between MLE and our LoRD. The results consistently show that LoRD significantly outperforms MLE under the same MEA settings. Besides, for challenging tasks such as reasoning and translation, LoRD exhibits much higher improvements, which demonstrates that it can address the preference overfitting problem discussed in Section 4.2 and do enable the local model to learn the task ability from victim models. However, we also observe that for some tasks (e.g., summarization), LoRD shows no statistical difference from MLE, probably because these tasks are relatively simple, where merely MLE has already achieved comparable results to victim models.
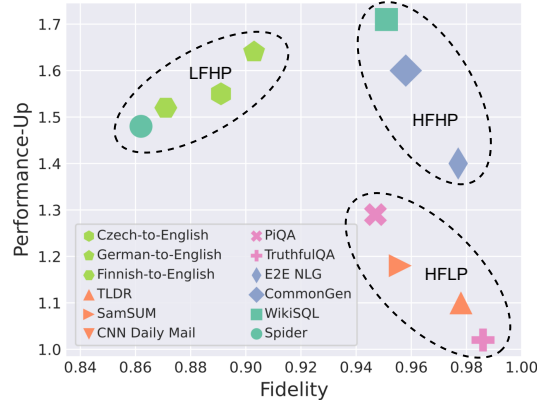

Figure 5: Spectrum of the fidelity and performance-up on extracting different downstream tasks. Current datasets can be divided into three groups: high fidelity and high performance-up (HFHP), high fidelity but low performance-up (HFLP), and low fidelity but high performance-up (LFHP).

Tasks difficulties comparison. Based on previous analysis, we observe that the performance and limitations of MEA depend on the category of tasks. Additionally, sometimes datasets in the same task exhibit significant differences in stealing. We put forward two metrics to measure task difficulties: the *fidelity* that measures extraction efficacy compared to victim models, and the *performance-up*, which assesses the performance gain before and after stealing for a given local model. Formally, given a test set $\mathcal{D}_{te} = \{(\mathbf{x}, \mathbf{y})\}$ and a corresponding metric $\mathcal{M}(hypothesis, reference)$, the fidelity ($F$) and performance-up ($P$) of the local model θ_{N_t} can be defined as:

$$F = \frac{\sum\limits_{\mathbf{x},\mathbf{y} \in \mathcal{D}_{te}} \mathcal{M}(\mathbf{y}_{N_t}, \mathbf{y})}{\sum\limits_{\mathbf{x},\mathbf{y} \in \mathcal{D}_{te}} \mathcal{M}(\mathbf{y}_{vic}, \mathbf{y})}, P = \frac{\sum\limits_{\mathbf{x},\mathbf{y} \in \mathcal{D}_{te}} \mathcal{M}(\mathbf{y}_{N_t}, \mathbf{y})}{\sum\limits_{\mathbf{x},\mathbf{y} \in \mathcal{D}_{te}} \mathcal{M}(\mathbf{y}_0, \mathbf{y})}, \tag{12}$$

where $\mathbf{y}_{N_t} \sim P_{\theta_{N_t}}(\cdot|\mathbf{x})$, $\mathbf{y}_0 \sim P_{\theta_0}(\cdot|\mathbf{x})$, and $\mathbf{y}_{vic} \sim P_{\theta_{vic}}(\cdot|\mathbf{x})$ denote the sampled responses from the trained local model (θ_{N_t}), the initial local model (θ_0), and the victim model (θ_{vic}), respectively. In Figure 5, we illustrate a "spectrum" of extracting various downstream tasks based on these two metrics defined in Equation 12. The figure can assist in recognizing and defending commercial LLM's knowledge.

From Figure 5, we observe five tasks forming the following three scenario groups and datasets coming from the same tasks are mostly in the same group:

- High fidelity and high performance-up (HFHP). These tasks are challenging for a pre-trained model but can be effectively learned with the guidance of victim models. This group includes two tasks: data-to-text and structured text generation.
- High fidelity but low performance-up (HFLP). The initial local model already achieves a comparable performance to the victim model. QAs and summarization are in this group.
- Low fidelity but high performance-up (LFHP). While MEAs significantly improve the local model's performance, gaps between the local and victim models remain difficult to bridge

with domain-specific extraction alone. Machine translation is a representative task whose reasons are explained in Section 5.2.

5.3 RESISTANCE TO WATERMARKS

Current LLM watermarking methods have been shown Kirchenbauer et al. (2023) to be robust against commonly used erasing strategies (e.g., rephrasing), making watermark removal a distinct challenge. In this section, we validate the inherent resistance of LoRD to watermarks, suggesting that LoRD is preliminarily resistant to text watermarking. As described in Section 4, we highlight that LoRD can extract the victim models' knowledge with two terms: the straightforward likelihood learning term $\log P_{\theta_t}(\mathbf{y}_{vic}|\mathbf{x}) - \log P_{\theta_t}(\mathbf{y}_{t-1}^-|\mathbf{x})$ and the exploration term $\log P_{\theta_t}(\mathbf{y}_{t-1}^+|\mathbf{x}) - \log P_{\theta_t}(\mathbf{y}_{t-1}^-|\mathbf{x})$, where we can tune the hyperparameter λ_1 as shown in $\mathcal{L}$ to trade off the exploration and the convergence speed. Typically, a lower λ_1 encourages the model for conducting a slower but more diverse and localized exploration from its own generated text $\mathbf{y}_{t-1}^+$, potentially enhancing watermark resistance. In this subsection, we evaluate this analysis empirically.

Watermarking Details. Unlike previous experimental settings in Section 5, here we cannot utilize commercial LLMs as victim models due to the inability to control token sampling inside LLMs. Instead, we employ Llama3-70B as the victim model and watermark its outputs based on *"green" tokens selection*. Following prior research Kirchenbauer et al. (2023), we separate the predicted vocabulary into a *green word set* and a *red word set* , assigning them randomly with the seed derived from the hash of generated tokens at the last generation step. Subsequently, we sample the next token **exclusively** from the green set, determined by a certain probability.

Figure 6: Comparison of watermarks resistance.

In this way, given the hypothesis H_0 that *texts are generated without the knowledge of the green word set*, we can estimate the probability H_0 occurs (*P-value*) and the *Z-score* of it for these texts. A high P-value, among with a low Z-score, indicates stronger watermark resistance for MEA algorithms.

Result Analysis. As depicted in Figure 6, we evaluate the watermark resistance for both MLE and LoRD, and demonstrate how LoRD's performance varies with different values of λ_1. The Z-score of LoRD witnesses a consistent increase as $\lambda 1$ arises, indicating that the "confidence" in rejecting the hypothesis, i.e., the risk to be suspected, arises when λ_1 increases. This finding coincides with the analysis in Section 4. Besides, we observe that the P-values of LoRD are generally higher than those of MLE when λ_1 is below 0.8, indicating that LoRD typically exhibits stronger watermarking resistance than MLE in most situations. It is noteworthy that this enhanced resistance seems not a "tax" of MEAs efficacy, as the Rouge-L (F1) scores of LoRD consistently surpass those of MLE and do not exhibit a significant negative correlation with their P-values.

6 CONCLUSION

In this paper, we have focused on the extraction problem of commercial large language models. We proposed LoRD, a practical and realistic extraction algorithm which is consistent with the alignment procedure of large language models. Our analysis proved that LoRD can reduce the query time significantly and mitigate the certification of current watermarks naturally, surpassing existing MEA algorithms' capabilities. Extensive experiments on domain-specific stealing demonstrated the superiority of our method.
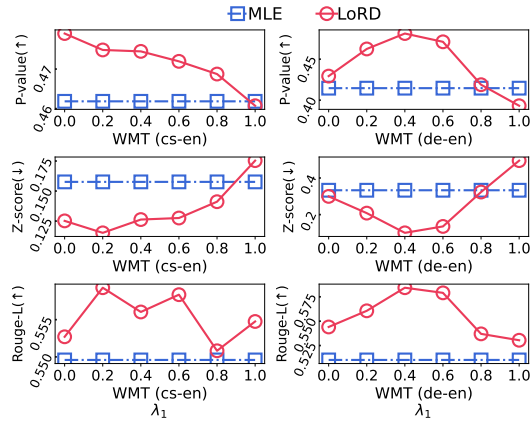
REFERENCES

Openai api reference documentation: chat. [Online]. https://platform.openai.com/docs/api-reference/chat.

Softmax doesn't work directly with nllloss, which expects the log to be computed between the softmax and itself. use log_softmax instead (it's faster and has better numerical properties). [Online]. https://pytorch.org/docs/stable/generated/torch.nn.functional.softmax.html#torch.nn.functional.softmax.

Chatgpt. [Online], 2024. https://chatgpt.com/.

Claude. [Online], 2024. https://claude.ai/.

Build the future of ai with meta llama 3. [Online], 2024. https://llama.meta.com/llama3/.

Josh Achiam, Steven Adler, Sandhini Agarwal, Lama Ahmad, Ilge Akkaya, Florencia Leoni Aleman, Diogo Almeida, Janko Altenschmidt, Sam Altman, Shyamal Anadkat, Red Avila, Igor Babuschkin, Suchir Balaji, Valerie Balcom, Paul Baltescu, Haiming Bao, Mohammad Bavarian, Jeff Belgum, Irwan Bello, Jake Berdine, Gabriel Bernadett-Shapiro, Christopher Berner, Lenny Bogdonoff, Oleg Boiko, Madelaine Boyd, and Anna-Luisa Brakman et al. Gpt-4 technical report, 2024. URL https://arxiv.org/abs/2303.08774.

Rohan Anil, Sebastian Borgeaud, Jean-Baptiste Alayrac, Jiahui Yu, Radu Soricut, Johan Schalkwyk, and Andrew M. Dai et al. Gemini: A family of highly capable multimodal models, 2024.

Yuntao Bai, Andy Jones, Kamal Ndousse, Amanda Askell, Anna Chen, Nova DasSarma, Dawn Drain, Stanislav Fort, Deep Ganguli, Tom Henighan, Nicholas Joseph, Saurav Kadavath, Jackson Kernion, Tom Conerly, Sheer El-Showk, and Nelson Elhage et al. Training a helpful and harmless assistant with reinforcement learning from human feedback, 2022a.

Yuntao Bai, Saurav Kadavath, Sandipan Kundu, Amanda Askell, Jackson Kernion, Andy Jones, Anna Chen, Anna Goldie, Azalia Mirhoseini, Cameron McKinnon, and Carol Chen et al. Constitutional AI: harmlessness from AI feedback. *CoRR*, abs/2212.08073, 2022b. doi: 10.48550/ARXIV.2212.08073. URL https://doi.org/10.48550/arXiv.2212.08073.

Michael Bailey, David Dittrich, Erin Kenneally, and Doug Maughan. The menlo report. *IEEE Security and Privacy*, 10(2):71–75, March 2012. ISSN 1540-7993. doi: 10.1109/MSP.2012.52. URL https://doi.org/10.1109/MSP.2012.52.

Yoshua Bengio, Réjean Ducharme, and Pascal Vincent. A neural probabilistic language model. *Advances in neural information processing systems*, 13, 2000.

Yonatan Bisk, Rowan Zellers, Ronan Le Bras, Jianfeng Gao, and Yejin Choi. Piqa: Reasoning about physical commonsense in natural language. In *Thirty-Fourth AAAI Conference on Artificial Intelligence*, 2020.

Ond rej Bojar, Rajen Chatterjee, Christian Federmann, Yvette Graham, Barry Haddow, Matthias Huck, Antonio Jimeno Yepes, Philipp Koehn, Varvara Logacheva, Christof Monz, Matteo Negri, Aurelie Neveol, Mariana Neves, Martin Popel, Matt Post, Raphael Rubino, Carolina Scarton, Lucia Specia, Marco Turchi, Karin Verspoor, and Marcos Zampieri. Findings of the 2016 conference on machine translation. In *Proceedings of the First Conference on Machine Translation*, pp. 131–198, Berlin, Germany, August 2016. Association for Computational Linguistics. URL http://www.aclweb.org/anthology/W/W16/W16-2301.

Tianshuo Cong, Xinlei He, and Yang Zhang. Sslguard: A watermarking scheme for self-supervised learning pre-trained encoders. In Heng Yin, Angelos Stavrou, Cas Cremers, and Elaine Shi (eds.), *Proceedings of the 2022 ACM SIGSAC Conference on Computer and Communications Security, CCS 2022, Los Angeles, CA, USA, November 7-11, 2022*, pp. 579–593. ACM, 2022. doi: 10.1145/3548606.3559355. URL https://doi.org/10.1145/3548606.3559355.

Jacob Devlin, Ming-Wei Chang, Kenton Lee, and Kristina Toutanova. BERT: Pre-training of deep bidirectional transformers for language understanding. In Jill Burstein, Christy Doran, and Thamar Solorio (eds.), *Proceedings of the 2019 Conference of the North American Chapter of the Association for Computational Linguistics: Human Language Technologies, Volume 1 (Long and Short Papers)*, pp. 4171–4186, Minneapolis, Minnesota, June 2019. Association for Computational Linguistics. doi: 10.18653/v1/N19-1423. URL `https://aclanthology.org/N19-1423`.

Ondřej Dušek, Jekaterina Novikova, and Verena Rieser. Evaluating the State-of-the-Art of End-to-End Natural Language Generation: The E2E NLG Challenge. *Computer Speech & Language*, 59: 123–156, January 2020. doi: 10.1016/j.csl.2019.06.009.

Amelia Glaese, Nat McAleese, Maja Trebacz, John Aslanides, Vlad Firoiu, Timo Ewalds, Maribeth Rauh, Laura Weidinger, Martin Chadwick, Phoebe Thacker, Lucy Campbell-Gillingham, Jonathan Uesato, Po-Sen Huang, Ramona Comanescu, and Fan Yang et al. Improving alignment of dialogue agents via targeted human judgements. *CoRR*, abs/2209.14375, 2022.

Bogdan Gliwa, Iwona Mochol, Maciej Biesek, and Aleksander Wawer. SAMSum corpus: A human-annotated dialogue dataset for abstractive summarization. In *Proceedings of the 2nd Workshop on New Frontiers in Summarization*, pp. 70–79, Hong Kong, China, November 2019. Association for Computational Linguistics. doi: 10.18653/v1/D19-5409. URL `https://www.aclweb.org/anthology/D19-5409`.

Xuanli He, Qiongkai Xu, Lingjuan Lyu, Fangzhao Wu, and Chenguang Wang. Protecting intellectual property of language generation apis with lexical watermark, 2021.

Xuanli He, Qiongkai Xu, Yi Zeng, Lingjuan Lyu, Fangzhao Wu, Jiwei Li, and Ruoxi Jia. CATER: intellectual property protection on text generation apis via conditional watermarks. In Sanmi Koyejo, S. Mohamed, A. Agarwal, Danielle Belgrave, K. Cho, and A. Oh (eds.), *Advances in Neural Information Processing Systems 35: Annual Conference on Neural Information Processing Systems 2022, NeurIPS 2022, New Orleans, LA, USA, November 28 - December 9, 2022*, 2022. URL `http://papers.nips.cc/paper_files/paper/2022/hash/2433fec2144ccf5fea1c9c5ebdbc3924-Abstract-Conference.html`.

Alex Heath. Bytedance is secretly using openai's tech to build a competitor. [Online], 2023. `https://www.theverge.com/2023/12/15/24003151/bytedance-china-openai-microsoft-competitor-llm`.

Karl Moritz Hermann, Tomás Kociský, Edward Grefenstette, Lasse Espeholt, Will Kay, Mustafa Suleyman, and Phil Blunsom. Teaching machines to read and comprehend. In *NIPS*, pp. 1693–1701, 2015. URL `http://papers.nips.cc/paper/5945-teaching-machines-to-read-and-comprehend`.

Geoffrey E. Hinton, Oriol Vinyals, and Jeffrey Dean. Distilling the knowledge in a neural network. *CoRR*, abs/1503.02531, 2015. URL `http://arxiv.org/abs/1503.02531`.

Ari Holtzman, Jan Buys, Li Du, Maxwell Forbes, and Yejin Choi. The curious case of neural text degeneration. *arXiv preprint arXiv:1904.09751*, 2019.

Matthew Jagielski, Nicholas Carlini, David Berthelot, Alex Kurakin, and Nicolas Papernot. High accuracy and high fidelity extraction of neural networks. In *29th USENIX Security Symposium (USENIX Security 20)*, pp. 1345–1362, 2020.

Hengrui Jia, Christopher A. Choquette-Choo, Varun Chandrasekaran, and Nicolas Papernot. Entangled watermarks as a defense against model extraction. In Michael D. Bailey and Rachel Greenstadt (eds.), *30th USENIX Security Symposium, USENIX Security 2021, August 11-13, 2021*, pp. 1937–1954. USENIX Association, 2021. URL `https://www.usenix.org/conference/usenixsecurity21/presentation/jia`.

John Kirchenbauer, Jonas Geiping, Yuxin Wen, Jonathan Katz, Ian Miers, and Tom Goldstein. A watermark for large language models. In Andreas Krause, Emma Brunskill, Kyunghyun Cho, Barbara Engelhardt, Sivan Sabato, and Jonathan Scarlett (eds.), *Proceedings of the 40th International Conference on Machine Learning*, volume 202 of *Proceedings of Machine Learning Research*, pp. 17061–17084. PMLR, 23–29 Jul 2023. URL `https://proceedings.mlr.press/v202/kirchenbauer23a.html`.

Robert Kirk, Ishita Mediratta, Christoforos Nalmpantis, Jelena Luketina, Eric Hambro, Edward Grefenstette, and Roberta Raileanu. Understanding the effects of rlhf on llm generalisation and diversity. *arXiv preprint arXiv:2310.06452*, 2023.

Kalpesh Krishna, Gaurav Singh Tomar, Ankur P. Parikh, Nicolas Papernot, and Mohit Iyyer. Thieves on sesame street! model extraction of bert-based apis. In *8th International Conference on Learning Representations, ICLR 2020, Addis Ababa, Ethiopia, April 26-30, 2020*. OpenReview.net, 2020. URL https://openreview.net/forum?id=Byl5NREFDr.

Harrison Lee, Samrat Phatale, Hassan Mansoor, Thomas Mesnard, Johan Ferret, Kellie Lu, Colton Bishop, Ethan Hall, Victor Carbune, Abhinav Rastogi, and Sushant Prakash. Rlaif: Scaling reinforcement learning from human feedback with ai feedback, 2023.

Zongjie Li, Chaozheng Wang, Pingchuan Ma, Chaowei Liu, Shuai Wang, Daoyuan Wu, Cuiyun Gao, and Yang Liu. On extracting specialized code abilities from large language models: A feasibility study, 2023.

Bill Yuchen Lin, Wangchunshu Zhou, Ming Shen, Pei Zhou, Chandra Bhagavatula, Yejin Choi, and Xiang Ren. CommonGen: A constrained text generation challenge for generative commonsense reasoning. In *Findings of the Association for Computational Linguistics: EMNLP 2020*, pp. 1823–1840, Online, November 2020. Association for Computational Linguistics. doi: 10.18653/v1/2020.findings-emnlp.165. URL https://www.aclweb.org/anthology/2020.findings-emnlp.165.

Chin-Yew Lin. ROUGE: A package for automatic evaluation of summaries. In *Text Summarization Branches Out*, pp. 74–81, Barcelona, Spain, July 2004. Association for Computational Linguistics. URL https://aclanthology.org/W04-1013.

Stephanie Lin, Jacob Hilton, and Owain Evans. Truthfulqa: Measuring how models mimic human falsehoods, 2021.

P. Lv, H. Ma, K. Chen, J. Zhou, S. Zhang, R. Liang, S. Zhu, P. Li, and Y. Zhang. Mea-defender: A robust watermark against model extraction attack. In *2024 IEEE Symposium on Security and Privacy (SP)*, pp. 102–102, Los Alamitos, CA, USA, may 2024. IEEE Computer Society. doi: 10.1109/SP54263.2024.00099. URL https://doi.ieeecomputersociety.org/10.1109/SP54263.2024.00099.

In Myung. Tutorial on maximum likelihood estimation. *Journal of Mathematical Psychology*, 47: 90–100, 02 2003. doi: 10.1016/S0022-2496(02)00028-7.

Long Ouyang, Jeff Wu, Xu Jiang, Diogo Almeida, Carroll L. Wainwright, Pamela Mishkin, Chong Zhang, Sandhini Agarwal, Katarina Slama, and Alex Ray et al. Training language models to follow instructions with human feedback. *ArXiv*, abs/2203.02155, 2022.

Nicolas Papernot, Patrick McDaniel, Ian Goodfellow, Somesh Jha, Z Berkay Celik, and Ananthram Swami. Practical black-box attacks against machine learning. In *Proceedings of the 2017 ACM on Asia conference on computer and communications security*, pp. 506–519, 2017.

Kishore Papineni, Salim Roukos, Todd Ward, and Wei-Jing Zhu. Bleu: a method for automatic evaluation of machine translation. In Pierre Isabelle, Eugene Charniak, and Dekang Lin (eds.), *Proceedings of the 40th Annual Meeting of the Association for Computational Linguistics*, pp. 311–318, Philadelphia, Pennsylvania, USA, July 2002. Association for Computational Linguistics. doi: 10.3115/1073083.1073135. URL https://aclanthology.org/P02-1040.

Wenjun Peng, Jingwei Yi, Fangzhao Wu, Shangxi Wu, Bin Bin Zhu, Lingjuan Lyu, Binxing Jiao, Tong Xu, Guangzhong Sun, and Xing Xie. Are you copying my model? protecting the copyright of large language models for EaaS via backdoor watermark. In Anna Rogers, Jordan Boyd-Graber, and Naoaki Okazaki (eds.), *Proceedings of the 61st Annual Meeting of the Association for Computational Linguistics (Volume 1: Long Papers)*, pp. 7653–7668, Toronto, Canada, July 2023. Association for Computational Linguistics. doi: 10.18653/v1/2023.acl-long.423. URL https://aclanthology.org/2023.acl-long.423.

Ethan Perez, Sam Ringer, Kamile Lukosiute, Karina Nguyen, Edwin Chen, Scott Heiner, Craig Pettit, Catherine Olsson, Sandipan Kundu, and et al. Discovering language model behaviors with model-written evaluations. In Anna Rogers, Jordan L. Boyd-Graber, and Naoaki Okazaki (eds.), *ACL 2023,*, pp. 13387–13434. Association for Computational Linguistics, 2023. doi: 10.18653/V1/2023.FINDINGS-ACL.847. URL `https://doi.org/10.18653/v1/2023.findings-acl.847`.

Rafael Rafailov, Archit Sharma, Eric Mitchell, Christopher D. Manning, Stefano Ermon, and Chelsea Finn. Direct preference optimization: Your language model is secretly a reward model. In Alice Oh, Tristan Naumann, Amir Globerson, Kate Saenko, Moritz Hardt, and Sergey Levine (eds.), *Advances in Neural Information Processing Systems 36: Annual Conference on Neural Information Processing Systems 2023, NeurIPS 2023, New Orleans, LA, USA, December 10 - 16, 2023*, 2023. URL `http://papers.nips.cc/paper_files/paper/2023/hash/a85b405ed65c6477a4fe8302b5e06ce7-Abstract-Conference.html`.

Mujahid Al Rafi, Yuan Feng, and Hyeran Jeon. Revealing secrets from pre-trained models. *CoRR*, abs/2207.09539, 2022. doi: 10.48550/ARXIV.2207.09539. URL `https://doi.org/10.48550/arXiv.2207.09539`.

David Saad and Sara Solla. Dynamics of on-line gradient descent learning for multilayer neural networks. *Advances in neural information processing systems*, 8, 1995.

John Schulman, Sergey Levine, Philipp Moritz, Michael I. Jordan, and Pieter Abbeel. Trust region policy optimization. *CoRR*, abs/1502.05477, 2015. URL `http://arxiv.org/abs/1502.05477`.

John Schulman, Filip Wolski, Prafulla Dhariwal, Alec Radford, and Oleg Klimov. Proximal policy optimization algorithms, 2017.

Noam Shazeer, Azalia Mirhoseini, Krzysztof Maziarz, Andy Davis, Quoc Le, Geoffrey Hinton, and Jeff Dean. Outrageously large neural networks: The sparsely-gated mixture-of-experts layer. *arXiv preprint arXiv:1701.06538*, 2017.

Rohan Taori, Ishaan Gulrajani, Tianyi Zhang, Yann Dubois, Xuechen Li, Carlos Guestrin, Percy Liang, and Tatsunori B. Hashimoto. Stanford alpaca: An instruction-following llama model. `https://github.com/tatsu-lab/stanford_alpaca`, 2023.

Yuandong Tian. Student specialization in deep rectified networks with finite width and input dimension. In *International Conference on Machine Learning*, pp. 9470–9480. PMLR, 2020.

Florian Tramèr, Fan Zhang, Ari Juels, Michael K Reiter, and Thomas Ristenpart. Stealing machine learning models via prediction apis. In *25th USENIX security symposium (USENIX Security 16)*, pp. 601–618, 2016.

Eric Wallace, Mitchell Stern, and Dawn Song. Imitation attacks and defenses for black-box machine translation systems. In Bonnie Webber, Trevor Cohn, Yulan He, and Yang Liu (eds.), *Proceedings of the 2020 Conference on Empirical Methods in Natural Language Processing, EMNLP 2020, Online, November 16-20, 2020*, pp. 5531–5546. Association for Computational Linguistics, 2020. doi: 10.18653/V1/2020.EMNLP-MAIN.446. URL `https://doi.org/10.18653/v1/2020.emnlp-main.446`.

Qiongkai Xu, Xuanli He, Lingjuan Lyu, Lizhen Qu, and Gholamreza Haffari. Student surpasses teacher: Imitation attack for black-box NLP apis. In *Proceedings of the 29th International Conference on Computational Linguistics, COLING 2022, Gyeongju, Republic of Korea, October 12-17, 2022*, pp. 2849–2860. International Committee on Computational Linguistics, 2022. URL `https://aclanthology.org/2022.coling-1.251`.

Tao Yu, Rui Zhang, Kai Yang, Michihiro Yasunaga, Dongxu Wang, Zifan Li, James Ma, Irene Li, Qingning Yao, Shanelle Roman, et al. Spider: A large-scale human-labeled dataset for complex and cross-domain semantic parsing and text-to-sql task. *arXiv preprint arXiv:1809.08887*, 2018.

Susan Zhang, Stephen Roller, Naman Goyal, Mikel Artetxe, Moya Chen, Shuohui Chen, Christopher Dewan, Mona Diab, Xian Li, Xi Victoria Lin, Todor Mihaylov, Myle Ott, Sam Shleifer, Kurt Shuster, Daniel Simig, Punit Singh Koura, Anjali Sridhar, Tianlu Wang, and Luke Zettlemoyer. Opt: Open pre-trained transformer language models, 2022.

Tianyi Zhang, Varsha Kishore, Felix Wu, Kilian Q. Weinberger, and Yoav Artzi. Bertscore: Evaluating text generation with BERT. In *8th International Conference on Learning Representations, ICLR 2020, Addis Ababa, Ethiopia, April 26-30, 2020*. OpenReview.net, 2020. URL `https://openreview.net/forum?id=SkeHuCVFDr`.

Xuandong Zhao, Lei Li, and Yu-Xiang Wang. Distillation-resistant watermarking for model protection in NLP. In Yoav Goldberg, Zornitsa Kozareva, and Yue Zhang (eds.), *Findings of the Association for Computational Linguistics: EMNLP 2022, Abu Dhabi, United Arab Emirates, December 7-11, 2022*, pp. 5044–5055. Association for Computational Linguistics, 2022. doi: 10.18653/V1/2022.FINDINGS-EMNLP.370. URL `https://doi.org/10.18653/v1/2022.findings-emnlp.370`.

Xuandong Zhao, Yu-Xiang Wang, and Lei Li. Protecting language generation models via invisible watermarking. In *Proceedings of the 40th International Conference on Machine Learning*, ICML'23. JMLR.org, 2023.

Victor Zhong, Caiming Xiong, and Richard Socher. Seq2sql: Generating structured queries from natural language using reinforcement learning. *CoRR*, abs/1709.00103, 2017.

Mo Zhou, Rong Ge, and Chi Jin. A local convergence theory for mildly over-parameterized two-layer neural network. In *Conference on Learning Theory*, pp. 4577–4632. PMLR, 2021.

A Ethical Considerations

As discussed in Section 1, MEAs are becoming increasingly prevalent in industrial settings and have already been executed, yet there remains a critical gap in understanding which specific tasks are more susceptible and what capabilities are necessary for effective executions. This lack of knowledge exacerbates the challenges faced by LLM maintainers in safeguarding their systems. Our research can contribute to that. Besides, the theoretical problem we address (as shown in Section 4) offers a novel and insightful perspective on the nature of this threat. Based on these two points, **we believe the benefits of our paper outweigh potential harms, which aligns with the principles of the *Menlo Report* Bailey et al. (2012) on ethics.** Additionally, we have submitted an anonymous version of the paper to the maintainers of the victim models used in our study to assist in improving their model security.

It is important to acknowledge, however, that the algorithms we propose could inadvertently enhance the efficiency of illicit extraction efforts by adversaries. To mitigate this risk, we have introduced and analyzed two defensive strategies in Appendix B, assessing both their effectiveness and potential vulnerabilities under adaptive attack scenarios. This ensures a comprehensive approach to bolstering the security of LLMs.

B Potential Defenses

Query Detection. One approach to effectively prevent the attack of LoRD is by detecting the distribution of query texts. This is because LoRD, similar to current MEA algorithms, makes no improvements to query samples, indicating that it can be detected by analyzing the statistical information of the adversary's queries, such as the number of queries, distribution of query contents, and so on. However, this defense is usually resource-consuming, as it requires the LLM provider to store all query texts of each user. Besides, the potential for false positives could adversely affect the user experience.

More Powerful Watermarks. While we highlight the watermark resistance of LoRD, watermarking remains one of the most effective solutions to mitigate MEAs. For example, some model-level watermarks, such as backdoor-based watermarking Jia et al. (2021); Lv et al. (2024), can effectively certify the theft of DNNs. However, model-level watermarking on LLMs remains preliminary. Besides, this technique might not work when the adversary only steals a subset of knowledge in which no backdoor is embedded.
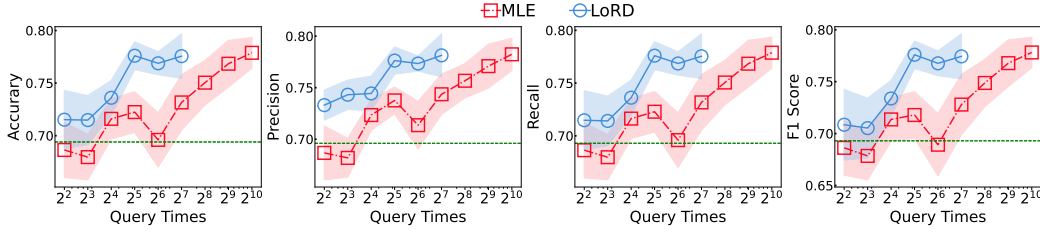
Figure 7: Comparison of query efficiency between MLE and LoRD on PiQA, where the *green horizontal line* represents the performance of the initialized local model. We increase query times for each method until reaching their bottlenecks. It can be found that the model extracted by LoRD typically performs a higher accuracy than MLE under the same number of queries. At the same time, LoRD reaches bottlenecks significantly earlier, reducing about 87% query cost compared with MLE.

C   SUPPLEMENTAL EXPERIMENTS

C.1   SCALING THE STEALING

In this subsection, we explore essential capacities to steal domain-specific knowledge from LLMs. We first analyze the influence of query times for the adversary, then compare the efficacy when utilizing different sizes of the local model, and finally compare the fidelity among different victim and local models.

C.1.1   QUERY TIMES

We first investigate the influence of query numbers on MEAs. Specifically, we sample query examples randomly from the query dataset, starting from 4, and incrementally increase it until the performance of the learned model stabilizes. Figure 7 illustrates the stealing efficacy of LoRD and MLE on PiQA.

We observe that the scores of MLE and LoRD consistently increase as the query number rises, showing that a larger query number can improve

Model/Metric	BLEU-1	BLEU-4	Rouge-L	BERTScore
Czech to English with 16 query samples				
Victim Model	0.611	0.313	0.604	0.957
Local Model	0.255	0.105	0.348	0.868
+MLE	0.535 ± 0.01	0.245 ± 0.01	0.526 ± 0.01	0.899 ± 0.00
+LoRD	0.545 ± 0.01	0.249 ± 0.00	0.538 ± 0.01	0.906 ± 0.00
German to English with 16 query sample				
Victim Model	0.661	0.377	0.652	0.965
Local Model	0.276	0.130	0.359	0.877
+MLE	0.578 ± 0.02	0.302 ± 0.01	0.573 ± 0.02	0.904 ± 0.01
+LoRD	0.587 ± 0.00	0.308 ± 0.00	0.589 ± 0.00	0.917 ± 0.00
Finnish to English with 16 query samples				
Victim Model	0.558	0.252	0.557	0.953
Local Model	0.242	0.085	0.320	0.866
+MLE	0.444 ± 0.03	0.173 ± 0.02	0.449 ± 0.03	0.905 ± 0.00
+LoRD	0.498 ± 0.01	0.196 ± 0.00	0.485 ± 0.01	0.905 ± 0.00

Table 2: MEA comparison on WMT16 Bojar et al. (2016) among MLE and our LoRD methods, where we use GPT-3.5-turbo as the victim model, and Llama3-8B lla (2024) as the local initial model.

stealing efficacy steadily until reaching their empirical upper bounds. Additionally, LoRD typically obtains a higher score than MLE with the same number of queries, and reaches bottlenecks earlier, which can reduce the required query numbers by 87% compared to MLE. Moreover, in Figure 7, the performance of LoRD exhibits a relatively lower standard variance than MLE, indicating a more stable training procedure.

C.1.2   SCALES OF LOCAL MODELS

As shown in our threat model (see Appendix F), we assume the adversary is stealing existing commercial LLMs with a small local model. This raises the question of selecting an appropriate interval of the local model's size. To address this concern, we illustrate the correlation between the local model's size and extraction efficacy on two machine translation tasks, Russian-to-English (ru-en) and German-to-English (de-en), as shown in Figure 8. Here, we employ seven OPT models Zhang et al. (2022) as local models, with parameters ranging from 125 million to 30 billion, to minimize the interruptions of factors other than model size.

Figure 8 shows a sharp distinction between two machine translation tasks. In the de-en task, the performance of the local model increases steadily with model size, while this trend is not evident in the ru-en task with model size smaller than 30 billion. Nevertheless, the performance of a
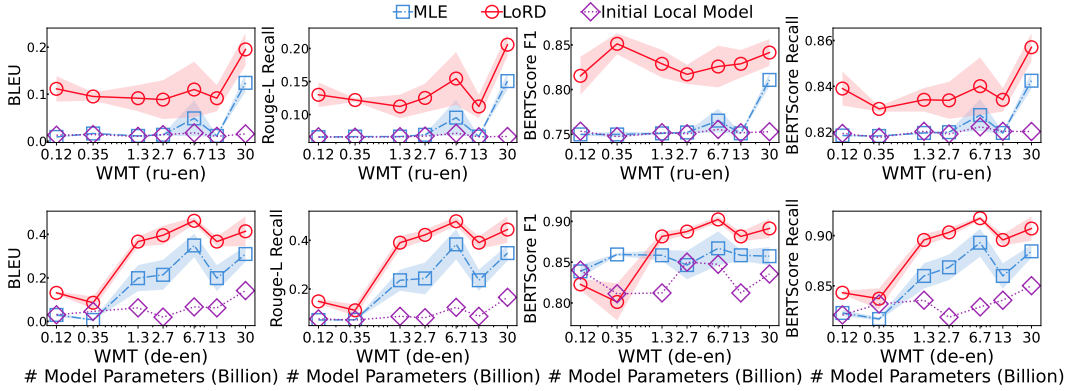
Figure 8: Experiments varying different model parameter scales.

30 billion parameter learned local model in ru-en cannot even be comparable to that of a 1.3 billion parameter local model in the de-en task. This phenomenon suggests that for tasks requiring commonsense knowledge, such as machine translation, the local model should at least possess foundational knowledge of the task (e.g., pre-trained on Russian texts) to learn from victim models effectively. Besides, experiments in BERTScore (F1) show that sometimes LoRD may underperform MLE when the local model has fewer than 1 billion parameters, demonstrating that it is challenging to bootstrap LoRD's exploration with a very small local model. By summarizing the increase in LoRD's curves, a model with 2.7 billion appears sufficient to steal domain-specific knowledge from commercial LLMs.

C.1.3 FIDELITY UNDER DIFFERENT VICTIM AND LOCAL MODELS

We then evaluate the fidelity of extracting different victim models using various pre-trained local models. Specifically, we select GPT-3.5, GPT-4, and GPT-4o as victim models, and employ five state-of-the-art open-source models, Phi-3 (3.8B), OPT (6.7B), Qwen-2 (7B), Mistral-V3 (7B), and Llama-3 (8B), as local models, as shown in Figure 9.

Horizontally, while GPT-4 exhibits a consistently lower extracted fidelity compared to the other two victim models, vulnerabilities of the three victim models are generally similar. Vertically, fidelity of different local models can be significantly impacted by their performance. For instance, OPT (6.7B) shows a noticeably lower score compared to the other four models, which indicates that the initial performance of the local model will affect the performance of MEAs. Besides, Phi-3 (3.8B) achieves a comparable fi-

Figure 9: Fidelity of extracted models with different victim models (GPT-3.5-turbo, GPT-4, and GPT-4o) and different local models (Phi-3, OPT, Qwen2, MistralV3, and Llama3).

delity to larger models like Llama-3 (8B), demonstrating that the size of a local model does not influence final fidelity in domain-specific stealing after 2.7 billion, which corroborates the observation in Appendix C.1.2.

C.2 VISUALIZATION OF DISTRIBUTIONS

We also investigate the *probability distributions* in the generation procedure among different extraction methods. Specifically, we visualize these distributions for four models, the victim model (GPT-3.5-turbo), the initial local model (llama3-8B), and the learned local models with MLE and LoRD.

As plotted in Figure 10, each row in the subfigures refers to the distribution when generating the i-th token, with each column element indicating the *probability* predicted for the corresponding token index. We limit the visualization to no more than five token probabilities as currently only GPT-3.5-turbo provides the token prediction probabilities during generation, with a maximum of 5 candidate tokens ope.

From Figure 10, we can see that both MLE and LoRD successfully redistribute the generation of the initial local model into a distribution similar to the victim model's, where probabilities, especially Top-1 tokens, have been well inherited in the extraction. This phenomenon supports our analysis in Proposition 2. However, distributions of MLE extracted models are consistently sharper than LoRD's, which aligns with our analysis in Section 4.2, where we claim that MLE leads local models to overfit to the preferred sentences (i.e., Top-1 tokens), namely *PO*, and thus to disrupt the original distributions, leveraging unusual low probabilities for other token indexes. The reason why LoRD can be resistant watermarks, i.e., tokens in Top-1, can also be derived from this discovery.

To compare MLE and LoRD accurately, we quantize the *entropy* of these distributions, and compute the *KL divergence* ($\mathbb{D}_{KL}$), and the
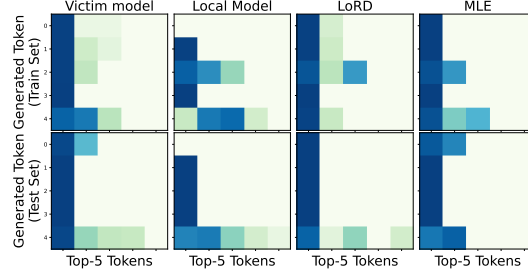

Figure 10: Token generation distributions of four models, namely the victim model, the (initial) local model, and the local model learned through LoRD and MLE, respectively. We visualize their logarithmic probability on examples sampled from the train set and test set, where a deeper color indicates a higher probability.

Spearman Correlation (Spear. Corr.) with respect to the victim and initial local model. As shown in Table 3, while the MLE extracted model exhibits a lower KL divergence (i.e., high distribution similarity) with the victim model than LoRD's on the training dataset, its KL divergence becomes comparable to LoRD's on the test set. Meanwhile, its Spearman correlation significantly decreases from 0.78 to 0.27, which shows that MLE cannot effectively imitate prediction behaviors of the victim model when encountering data beyond the training dataset.

D PROOFS

D.1 PROOFS OF PROPOSITION 1

As we described in Section 2, both existing methods and LoRD are learned from the victim model's response $\mathbf{y}_{vic}$ and the corresponding probability distribution $P_{\theta_{vic}}(\cdot|\mathbf{x}) \in \mathbb{R}^V$, where V denotes the vocabulary size. Therefore, we first investigate how the local model is learned to emulate the distribution of the victim model, $P_{\theta_{vic}}(\cdot|\mathbf{x})$, under the following three stealing strategies.

Expected Distribution of MLE. We can first reshape the MLE loss into a special formation of Kullback-Leibler divergence with labels of one-hot distributions, that is,

Models\Metrics	Entropy	To Victim Model		To Initial Local Model	
		$\mathbb{D}_{KL}\downarrow$	Spear. Corr.↑	$\mathbb{D}_{KL}$	Spear. Corr.
On training dataset					
Initial Local Model	0.395	0.503	0.620	-	-
+ LoRD	0.209	0.051	**0.880**	0.169	0.680
+ MLE	0.271	**0.029**	0.780	0.051	0.540
On the test dataset					
Initial Local Model	0.269	0.471	0.680	-	-
+ LoRD	0.122	0.033	**0.640**	0.046	0.720
+MLE	0.275	**0.032**	0.274	0.001	0.740

Table 3: Quantization analysis on distributions. A low KL divergence or a high Spearman correlation indicates a high similarity.

$$\mathcal{L}_{ce} = - \sum_{\mathbf{x},\mathbf{y}\sim\mathcal{D}_{tr}} \log P_\theta(\mathbf{y}_{vic}|\mathbf{x}) = \sum_{\mathbf{x},\mathbf{y}\sim\mathcal{D}_{tr}} \sum_j^N \mathbb{D}_{KL}[\mathbf{1}_{y_{vic,j}}||P_\theta(\cdot|\mathbf{x},\mathbf{y}_{vic,<j})], \qquad (13)$$

where $\mathbf{1}_{y_{vic,j}}$ is a one-hot vector in which only $\mathbf{1}_{y_{vic,j}}[y_{vic,j}] = 1$ and all the other elements are 0. Equation 13 demonstrates that MLE learns to maximize the probability of $\mathbf{y}_{vic,j}$, without explicit constraints on probabilities across other dimensions.
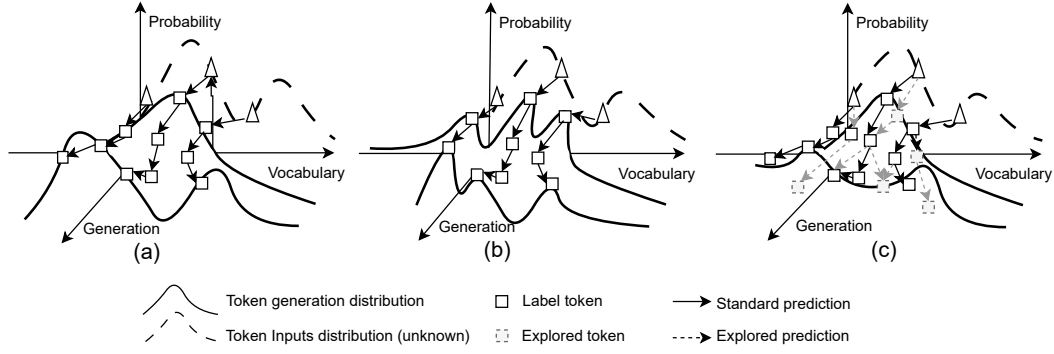
Figure 11: Comparison of learned joint *prediction distributions* among the victim model (a), local models are learned with MLE (b) and LoRD (c). Simply obtaining the tokens from the victim model (solid black squares), MLE may only memorize specific responses and build a complicated decision surface, resulting in *preference overfitting*. In contrast, LoRD further explores the candidate generation paths (dashed arrows and squares) under the guidance of the victim's generation, which is expected to better approximate the victim model in terms of generalization ability, especially under a limited query budget.

Expected Distribution of KD. Following a previous work Hinton et al. (2015), the objective function of KD is

$$\mathcal{L}_{kd} = \mathbb{D}_{KL}[P_{\theta_{vic}}(\cdot|\mathbf{x})||P_\theta(\cdot|\mathbf{x})] + T^2 \cdot \mathbb{D}_{KL}[\text{SM}(P_{\theta_{vic}}(\cdot|\mathbf{x})/T)||\text{SM}(P_\theta(\cdot|\mathbf{x})/T)], \quad (14)$$

where $\text{SM}(\cdot)$ represents the *softmax function*, and $T > 1$ denotes the temperature to smooth the targeted distribution $P_{\theta_{vic}}(\cdot|\mathbf{x})$. As described in Equation 14, knowledge distillation aims to align $P_\theta(\cdot|\mathbf{x})$ with $P_{\theta_{vic}}(\cdot|\mathbf{x})$ in both the original and the smoothed probability across all dimensions, which is exceptionally comprehensive among these methods.

Expected Distribution of Alignments. Replacing Equation 6 with Equation 5, we can merge the optimization target of LLMs' alignments as

$$\min_{\theta*} - \sum_{(\mathbf{x},\mathbf{y}^+,\mathbf{y}^-)\sim\mathcal{D}^{pref}} \sigma\left(\log\frac{P_{\theta*}(\mathbf{y}^+|\mathbf{x})/P_{\theta*}(\mathbf{y}^-|\mathbf{x})}{P_{\theta_{init}}(\mathbf{y}^+|\mathbf{x})/P_{\theta_{init}}(\mathbf{y}^-|\mathbf{x})}\right)$$
$$\Rightarrow \max_{\theta*} \sum_{(\mathbf{x},\mathbf{y}^+,\mathbf{y}^-)\sim\mathcal{D}^{pref}} \log P_{\theta*}(\mathbf{y}^+|\mathbf{x}) - \log P_{\theta*}(\mathbf{y}^-|\mathbf{x}), \quad (15)$$

where $\theta*$ denotes the expected parameters of the models as

$$P_{\theta*}(\mathbf{y}|\mathbf{x}) = \frac{1}{Z(x)} P_{\theta_{init}}(\mathbf{y}|\mathbf{x}) \cdot e^{\frac{1}{\beta}R_\phi(\mathbf{x},\mathbf{y})}. \quad (16)$$

We provide a detailed derivation for Equation 16 in Appendix D.2. By replacing Equation 15 with Equation 16, the expected distribution can be represented as $\mathbf{r}_{i,j}\cdot P_{\theta_{init}}(\cdot|\mathbf{x})$, in which $\mathbf{r}_{i,j}$ indicates the wrapped distribution gain. This distortion aims to maximize the ratio $P_\theta(y_j^+|\mathbf{x},\mathbf{y}_{<j}^+)/P_\theta(y_j^-|\mathbf{x},\mathbf{y}_{<j}^+)$, and leave the probabilities in other dimensions unconstrained directly.

Expected Distribution of LoRD. Similar to alignments, the expected converging procedure by the objective function $\mathcal{L}_{obj}$ is also intended to maximize the ratio between positive samples and negative samples, i.e., $P_{\theta_t}(\mathbf{y}_{t-1}^+|\mathbf{x})/P_{\theta_t}(\mathbf{y}_{t-1}^-|\mathbf{x})$. Meanwhile, the regularization term $P_{\theta_t}(\mathbf{y}_{vic}|\mathbf{x})/P_{\theta_t}(\mathbf{y}_{t-1}^-|\mathbf{x})$ will guide the models to maximize the ratio between $\mathbf{y}_{vic}$ and $\mathbf{y}_{t-1}^-$. As the "standard response" to be learned, $\mathbf{y}_{vic}$ can be viewed sufficiently as a positive example. Therefore, we can derive that the optimization target of LoRD is consistent with RLHF's optimization, i.e., both encourage local models to maximize the probability proportion between positive and negative samples.

Similar to Equation 16 in which the optimized model can be seen as the distortion of the original model $P_{\theta_{init}}$, in LoRD the optimized model can be regarded as the distortion of the local model P_{θ_0}, with $P_{\theta_t}(\cdot|\mathbf{x}) = \mathbf{r}_{i,j}^t P_{\theta_{t-1}}(\cdot|\mathbf{x})$ at each step t, where the distortion term $\mathbf{r}_{i,j}^t$ is intended to jointly maximize $P_{\theta_t}(\mathbf{y}_{t-1}^+|\mathbf{x})/P_{\theta_t}(\mathbf{y}_{t-1}^-|\mathbf{x})$ and $P_{\theta_t}(\mathbf{y}_{vic}|\mathbf{x})/P_{\theta_t}(\mathbf{y}_{t-1}^-|\mathbf{x})$, while leaving the probabilities in other dimensions unconstrained directly.

D.2 THE DEDUCTION OF EQUATION 16 IN PROPOSITION 1

From Equation 6, we can get that

$$\max_{\theta} \sum_{\mathbf{x} \sim \mathcal{D}_q} R_{\theta_\phi}(\mathbf{x}, \hat{\mathbf{y}}) - \beta \mathbb{D}_{KL}[P_\theta(\mathbf{y}|\mathbf{x})||P_{\theta_{init}}(\mathbf{y}|\mathbf{x})]$$

$$\Rightarrow \max_{\theta} \sum_{\mathbf{x} \sim \mathcal{D}_q} \sum_{\mathbf{y} \sim P_\theta(\cdot|\mathbf{x})} R_{\theta_\phi}(\mathbf{x}, \mathbf{y}) - \beta[\log P_\theta(\mathbf{y}|\mathbf{x}) - \log P_{\theta_{init}}(\mathbf{y}|\mathbf{x})]$$

$$\Rightarrow \min_{\theta} \sum_{\mathbf{x} \sim \mathcal{D}_q} \sum_{\mathbf{y} \sim P_\theta(\cdot|\mathbf{x})} -\frac{1}{\beta} R_{\theta_\phi}(\mathbf{x}, \mathbf{y}) + \log \frac{P_\theta(\mathbf{y}|\mathbf{x})}{P_{\theta_{init}}(\mathbf{y}|\mathbf{x})}$$

$$\Rightarrow \min_{\theta} \sum_{\mathbf{x} \sim \mathcal{D}_q} \sum_{\mathbf{y} \sim P_\theta(\cdot|\mathbf{x})} -\log(\exp(\frac{1}{\beta} R_{\theta_\phi}(\mathbf{x}, \mathbf{y}))) + \log \frac{P_\theta(\mathbf{y}|\mathbf{x})}{P_{\theta_{init}}(\mathbf{y}|\mathbf{x})}$$

$$\Rightarrow \min_{\theta} \sum_{\mathbf{x} \sim \mathcal{D}_q} \sum_{\mathbf{y} \sim P_\theta(\cdot|\mathbf{x})} \log \frac{P_\theta(\mathbf{y}|\mathbf{x})}{\exp(\frac{1}{\beta} R_{\theta_\phi}(\mathbf{x}, \mathbf{y})) \cdot P_{\theta_{init}}(\mathbf{y}|\mathbf{x})}.$$

If we define a partition function $Z(\mathbf{x})$ with the formation of

$$Z(\mathbf{x}) = \sum_{\mathbf{y}} P_{init}(\mathbf{y}|\mathbf{x}) \exp(\frac{1}{\beta} R_{\theta_\phi}(\mathbf{x}, \mathbf{y})), \tag{17}$$

we can reformat the optimization target as

$$\min_{\theta} \sum_{\mathbf{x} \sim \mathcal{D}_q} \sum_{\mathbf{y} \sim P_\theta(\cdot|\mathbf{x})} \log \frac{P_\theta(\mathbf{y}|\mathbf{x})}{\exp(\frac{1}{\beta} R_{\theta_\phi}(\mathbf{x}, \mathbf{y})) \cdot P_{\theta_{init}}(\mathbf{y}|\mathbf{x})}$$

$$\Rightarrow \min_{\theta} \sum_{\mathbf{x} \sim \mathcal{D}_q} \sum_{\mathbf{y} \sim P_\theta(\cdot|\mathbf{x})} \log \frac{Z(\mathbf{x}) \cdot P_\theta(\mathbf{y}|\mathbf{x})}{\exp(\frac{1}{\beta} R_{\theta_\phi}(\mathbf{x}, \mathbf{y})) \cdot P_{\theta_{init}}(\mathbf{y}|\mathbf{x})}$$

$$- \log Z(\mathbf{x}).$$

If we mark $\frac{1}{Z(\mathbf{x})} \exp(\frac{1}{\beta} R_{\theta_\phi}(\mathbf{x}, \mathbf{y})) \cdot P_{\theta_{init}}(\mathbf{y}|\mathbf{x})$ as $P_{\theta*}(\mathbf{y}|\mathbf{x})$, then we have

$$\min_{\theta} \sum_{\mathbf{x} \sim \mathcal{D}_q} \sum_{\mathbf{y} \sim P_\theta(\cdot|\mathbf{x})} \log \frac{Z(\mathbf{x}) \cdot P_\theta(\mathbf{y}|\mathbf{x})}{\exp(\frac{1}{\beta} R_{\theta_\phi}(\mathbf{x}, \mathbf{y})) \cdot P_{\theta_{init}}(\mathbf{y}|\mathbf{x})} - \log Z(\mathbf{x})$$

$$\Rightarrow \min_{\theta} \sum_{\mathbf{x} \sim \mathcal{D}_q} \sum_{\mathbf{y} \sim P_\theta(\cdot|\mathbf{x})} \log \frac{P_\theta(\mathbf{y}|\mathbf{x})}{P_{\theta*}(\mathbf{y}|\mathbf{x})} - \log Z(\mathbf{x}).$$

Because $Z(\mathbf{x})$ is independent to $\mathbf{y}$, we can deduct that

$$\min_{\theta} \sum_{\mathbf{x} \sim \mathcal{D}_q} \sum_{\mathbf{y} \sim P_\theta(\cdot|\mathbf{x})} \log \frac{P_\theta(\mathbf{y}|\mathbf{x})}{P_{\theta*}(\mathbf{y}|\mathbf{x})} - \log Z(\mathbf{x})$$

$$\Rightarrow \min_{\theta} \sum_{\mathbf{x} \sim \mathcal{D}_q} \left[\sum_{\mathbf{y} \sim P_\theta(\cdot|\mathbf{x})} \log \frac{P_\theta(\mathbf{y}|\mathbf{x})}{P_{\theta*}(\mathbf{y}|\mathbf{x})} \right] - \log Z(\mathbf{x}) \tag{18}$$

$$\Rightarrow \min_{\theta} \sum_{\mathbf{x} \sim \mathcal{D}_q} \mathbb{D}_{KL}[P_\theta(\mathbf{y}|\mathbf{x})||P_{\theta*}(\mathbf{y}|\mathbf{x})] - \log Z(\mathbf{x}).$$

As we know that $Z(\mathbf{x})$ does not contain θ, the above optimization target actually minimizes the KL-divergence between the distribution of P_θ and $P_{\theta*}$, demonstrating that $\theta*$ is the optimal value of θ that satisfies

$$P_{\theta*}(\mathbf{y}|\mathbf{x}) = \frac{1}{Z(\mathbf{x})} \exp(\frac{1}{\beta} R_{\theta_\phi}(\mathbf{x}, \mathbf{y})) \cdot P_{\theta_{init}}(\mathbf{y}|\mathbf{x}). \tag{19}$$

Based on equation 19, we can see that the optimal distribution of θ is built upon $P_{\theta_{init}}$ with a distortion, as we discussed in Section 4.1.

D.3 PROOFS OF PROPOSITION 2

Guarantee of MLE. From Equation 13 we can obtain that when $\mathcal{L}_{ce}$ decreases to 0, the KL divergence between $P_\theta(\cdot|\mathbf{x})$ and $P_{\theta_{vic}}(\cdot|\mathbf{x})$ decreases to 0, indicating that $P_\theta(\cdot|\mathbf{x})$ equals to $P_{\theta_{vic}}(\cdot|\mathbf{x})$.

Guarantee of KD. As we know, $\mathbb{D}_{KL}(p, q) \geq 0 \; \forall \; p$ and q. Therefore, if $\mathcal{L}_{kd}$ shown in Equation 14 equals to 0, then both $\mathbb{D}_{KL}[P_\theta(\cdot|\mathbf{x})||P_{\theta_{vic}}(\cdot|\mathbf{x})]$ and $\mathbb{D}_{KL}[\text{SM}(P_\theta(\cdot|\mathbf{x})/T)||\text{SM}(P_{\theta_{vic}}(\cdot|\mathbf{x})/T)]$ equal to 0. For the latter one, we have

$$\mathbb{D}_{KL}[\text{SM}(P_{\theta_{vic}}(\cdot|\mathbf{x})/T)||\text{SM}(P_\theta(\cdot|\mathbf{x})/T)]$$

$$= \mathbb{E}_{\mathbf{y}\sim P_{\theta_{vic}}(\cdot|\mathbf{x})}\mathbb{E}_{y\in\mathbf{y}}\left[\log\frac{\exp(P_\theta(y|\mathbf{x},\mathbf{y}_p)/T)/\sum_{y'\in\mathbf{y}}\exp(P_{\theta_{vic}}(y|\mathbf{x},\mathbf{y}_p)/T)}{\exp(P_{\theta_{vic}}(y|\mathbf{x},\mathbf{y}_p)/T)/\sum_{y'\in\mathbf{y}}\exp(P_\theta(y|\mathbf{x},\mathbf{y}_p)/T)}\right]$$

$$= \mathbb{E}_{\mathbf{y}\sim P_{\theta_{vic}}(\cdot|\mathbf{x})}\mathbb{E}_{y\in\mathbf{y}}\left[\log\frac{\exp((P_\theta(y|\mathbf{x},\mathbf{y}_p) - P_{\theta_{vic}}(y|\mathbf{x},\mathbf{y}_p))/T)}{\sum_{y'\in\mathbf{y}}\exp(P_{\theta_{vic}}(y|\mathbf{x},\mathbf{y}_p)/T)/\sum_{y'\in\mathbf{y}}\exp(P_\theta(y|\mathbf{x},\mathbf{y}_p)/T)}\right],$$

where we can observe that only when $P_\theta(\cdot|\mathbf{x})$ equals to $P_{\theta_{vic}}(\cdot|\mathbf{x})$ can this term reduce to 0. Integrating the analysis of these two terms, we can obtain that $\mathcal{L}_{kd} = 0$ represents the local model's distribution converge to that of the victim model.

Guarantee of LoRD. When $\mathcal{L}$ shown in Equation 11 equals to 0, the proportion of $P_{\theta_t}(\mathbf{y}_{vic}|\mathbf{x})/P_{\theta_t}(\mathbf{y}_{t-1}^-|\mathbf{x})$ and $P_{\theta_t}(\mathbf{y}_{t-1}^+|\mathbf{x})/P_{\theta_t}(\mathbf{y}_{t-1}^-|\mathbf{x})$ should limit to $-\infty$. As we know that *i)* in a distribution $\sum P_{\theta_t}(\cdot|\mathbf{x}) = 1$ and *ii)* $\mathbf{y}_{t-1}^+$ is a dynamic positive response generated at each period, we can deduct that when $\mathcal{L} = 0$ there must be $\mathbf{y}_{vic} = \mathbf{y}_{t-1}^+$, i.e., $P_{\theta_t}(\mathbf{y}_{vic}|\mathbf{x}) = P_{\theta_t}(\mathbf{y}_{t-1}^+|\mathbf{x}) = 1$ and $P_{\theta_t}(\mathbf{y}_{t-1}^-|\mathbf{x}) = 0$. Note that this is merely a theoretical limit that cannot be reached, because $\mathbf{y}_{t-1}^-$ will not be sampled if its probability is 0, and $\mathbf{y}_{t-1}^+$ usually doesn't exhibit a significant distinction to $\mathbf{y}_{t-1}^-$ when sampling.

E SUPPLEMENTAL RELATED WORKS

E.1 HUMAN-FEEDBACK-FREE ALIGNMENTS

There are several alternatives to the standard RLHF approach. Lee et al. (2023) propose reinforcement learning with AI feedback (RLAIF) as a means to diminish the annotation burden associated with the preference assessments. Besides, there are some approaches, such as direct preference optimization (DPO) Rafailov et al. (2023), that conceptualize the language model itself as the reward model and thus consolidate Equation 5 and Equation 6 into a unified supervised and preference-based training task. Since they do not change the primary targets (i.e., maximizing rewards) and optimization strategies of LLM's alignments, we only consider the standard formation of alignments for simplicity in our theoretical analysis.

E.2 LANGUAGE MODELS EXTRACTION

Studies to steal language models originated from the natural language understanding (NLU) models, such as BERTDevlin et al. (2019), and then evolved to generative language models, especially large language models recently.

Krishna et al. (2020) highlights early recognition of model extraction threats in language models. By constructing text inputs with randomly vocabulary sampling, they successfully extract the weights from BERT-based APIs. Besides, Rafi et al. (2022) investigate the feasibility of side-channel model extraction attacks, revealing that by analyzing extra signals from GPU kernels, one could accurately steal the model architecture and its parameters. Subsequent research Xu et al. (2022) has thoroughly investigated the strategy of ensembling victim models to train a competitor model that surpasses its teachers.

Datasets\ Models	Links
PIQA	https://huggingface.co/datasets/piqa
TruthfulQA	https://huggingface.co/datasets/truthful_qa
WMT16	https://huggingface.co/datasets/wmt16
E2E NLG	https://huggingface.co/datasets/e2e_nlg
CommonGen	https://huggingface.co/datasets/allenai/common_gen
WikiSQL	https://huggingface.co/datasets/wikisql
Spider	https://huggingface.co/datasets/spider
TLDR	https://huggingface.co/datasets/UCL-DARK/openai-tldr-filtered
SamSUM	https://huggingface.co/datasets/samsum
CNN Daily Mail	https://huggingface.co/datasets/cnn_dailymail
Llama3-8B	https://huggingface.co/meta-llama/Meta-Llama-3-8B-Instruct
Llama3-70B	https://huggingface.co/meta-llama/Meta-Llama-3-70B-Instruct
Phi3-3.8B	https://huggingface.co/microsoft/Phi-3-mini-4k-instruct
OPT-6.7B	https://huggingface.co/facebook/opt-6.7b
Qwen2-7B	https://huggingface.co/Qwen/Qwen2-7B-Instruct
MistralV3-7B	https://huggingface.co/mistralai/Mistral-7B-Instruct-v0.3

Table 4: Datasets and pre-trained model checkpoints used in the paper.

The exploration of generative language model extraction is still in its infant stage, with only a handful of studies thus far. Wallace et al. (2020) investigate imitation attacks on natural language models. By designing monolingual query texts and collecting responses, they successfully extract the knowledge from a simulated machine translation model under the black-box settings. This research exhibits that slight architectural differences will not influence the extraction between language models. Li et al. (2023) also explores the potential risks of stealing the code-generation abilities of LLMs into smaller downstream models. Unlike previous research Wallace et al. (2020), this is the first study that selects LLMs as targets. By collecting large-scale domain-specific samples, they fine-tune a 7-billion local pre-trained model with them and show the similarity between the victim and local models in both performances and adversarial samples. However, these two studies employ the MLE loss (Equation 3) as the MEA method, neither considering whether MLE is compatible with LLMs's training, especially the alignment procedure shown in Section 2.2, nor addressing optimizations related to query efficiency and the watermark resistance. Besides, the scope of these studies is limited to stealing specific knowledge in a few downstream domains. At the same time, most of the critical aspects of LLMs and the required extraction capabilities, such as query numbers and local model scales, remain unresolved.

E.3 TEXT WATERMARKS

In contrast to stealing LLMs, IP protection methods have received considerable attention recently. By sampling a stealthy but representative "greed word set" on the vocabulary distribution, these methods Cong et al. (2022); He et al. (2022; 2021); Kirchenbauer et al. (2023) can remap the generated words into their synonyms or add the "watermarked" token automatically, and thus effectively certify the output. Besides, strategies such as integrating embeddings into the representation as the backdoor Peng et al. (2023) or manipulating the probabilities with crafted sinusoidal noises Zhao et al. (2022; 2023) are also proposed. However, these approaches often presume more stringent conditions regarding the victim and the suspected models. This paper will further assess the effectiveness of LoRD and current MEAs in evading these black-box watermarking strategies.

F A DETAILED THREAT MODEL

Adversary's Objective. The adversary's objective is to steal the targeted knowledge from LLMs. Specifically, we select machine translation, reasoning, data-to-text, structured text generation, and summarization as the downstream domain-specific tasks. The adversary aims to develop a *query-efficient* MEA algorithm, since the amount of input and generated tokens will be counted as the costs. Additionally, the MEA methods are expected to be *watermark-resistant*, i.e., they are highly desired to reduce the risks of exposure to unauthorized stealing.

Targeted Models. We select Llama3-70B, GPT-3.5-turbo, and GPT-4o as the victim models in this paper. Unlike previous works that only deployed simulated local victim models (e.g., OPT Zhang et al. (2022)), our selections aim to expose the stealing threat on realistic AI services. Besides, our

Model/Metric	Accuracy	Precision	Recall	F1 Score
PIQA Bisk et al. (2020) with 64 query samples				
Victim Model	0.828	0.828	0.827	0.827
Local Model	0.622	0.638	0.621	0.609
+MLE (baseline)	0.760 ± 0.02	0.771 ± 0.01	0.760 ± 0.02	0.757 ± 0.03
+KD (gre-box)	0.759 ± 0.02	0.760 ± 0.02	0.759 ± 0.02	0.759 ± 0.02
+LoRD (ours)	0.785 ± 0.01	0.795 ± 0.01	0.785 ± 0.01	0.783 ± 0.02
TruthfulQA Lin et al. (2021) with 64 query samples				
Victim Model	0.414	0.500	0.207	0.293
Local Model	0.391	0.500	0.195	0.281
+MLE (baseline)	0.381 ± 0.17	0.500 ± 0.00	0.190 ± 0.09	0.266 ± 0.09
+KD (gre-box)	0.463 ± 0.03	0.500 ± 0.00	0.232 ± 0.01	0.316 ± 0.01
+LoRD (ours)	0.408 ± 0.05	0.500 ± 0.00	0.204 ± 0.03	0.289 ± 0.03

Table 5: MEA comparison on QA tasks among MLE and our LoRD methods, where we use GPT-3.5-turbo as the victim model, and Llama3-8B lla (2024) as the local initial model.

Task	Instruction
WMT16	Please translate the sentence from [source language] to English.
PiQA & TruthfulQA	Please select the correct answer for the "Question" of Users. Question: [question] Selection 1: [Selection1] Selection 2:[Selection2].
E2E NLG	Please translate the information to a sentence in natural language.
CommonGen	Please generate a sentence based on the words provided by Users.
WikiSQL& Spider	Please return to me the SQL sentence based on the text (i.e., Question) and the table information (i.e., Table) provided by the User.
TLDR& SamSUM	Please **summarize** the content given by the user.
CNN Daily Mail	Please **summarize** the content given by the user.

Table 6: Instructions used in the different downstream datasets.

target models are specifically constrained to LLMs fine-tuned with alignment methods (e.g., RLHF) since they are not only state-of-the-art solutions now but also more valuable due to their human-based alignments.

Adversary's Capabilities. In accordance with the LLM-based AI service APIs, we identify two attack scenarios: black-box and grey-box attacks. In the black-box scenario, only textual responses the adversary is allowed to obtain. At the same time, all other information, such as the temperature, sampling strategies, and the hidden states of LLMs, are unseen and inaccessible. On the contrary, a grey-box attack allows the adversary to access the generation probabilities distribution of tokens. Notice that both MLE and our LoRD method are under black-box settings, and we only adopt grey-box settings on some particular stealing methods, such as knowledge distillation.

Besides, this paper posits that the adversary usually has worse training conditions than the victims. Specifically, query times and the scale of the local model available to the adversary are much smaller than the victims' training datasets and model parameters. This setting has been adopted in previous LLMs' extraction Li et al. (2023). We call it a LaViSH (**La**rge-**Vi**ctim-**S**mall-**H**eist) framework, which allows us to estimate the upper bound of MEA risks empirically. For adversaries with more substantial resources, they can train more powerful MEA-based LLMs by leveraging MEA algorithms under our LaViSH settings.

G   LIMITATIONS AND FUTURE WORKS

MEAs on Multi-modal Models. While this paper delves into MEAs for large language models, it acknowledges the oversight of the multi-modal attribution of current commercial models Anil et al. (2024); Achiam et al. (2024) that integrate various forms of data such as text, images, voice, and so on. The challenge of extending MEA algorithms to accommodate these models, which requires extra considerations on the unified representation of concepts, remains unexplored. Future work could focus on developing MEA methodologies sensitive to multi-modal data nuances.

Capacities beyond LaViSH Settings. We utilize the LaViSH setting to describe the model capacity of adversaries in our threat model (see Appendix F). However, sometimes, the adversary might possess comparable or superior training resources to the victims. Though this paper posits that our

---

Algorithm 1 LoRD Algorithm

1: **Input:** Query dataset $\mathcal{D}_q$, local language model θ_{init}, interface of the victim model $P_{\theta_{vic}}(\cdot|\cdot)$, train period number N_t, threshold values τ_1 and τ_2.
2: // Initialization.
3: $\theta_0 \leftarrow \theta_{init}, \mathcal{D}_{tr} \leftarrow \emptyset, \mathcal{D}_0^+ \leftarrow \emptyset, \mathcal{D}_0^- \leftarrow \emptyset, t \leftarrow 0;$
4: // Query the victim model.
5: **for** $\mathbf{x} \sim \mathcal{D}_q$ **do**
6:    $\mathbf{y}_{vic} \leftarrow P_{\theta_{vic}}(\cdot|\mathbf{x});$
7:    $\mathcal{D}_{tr} \leftarrow \mathcal{D}_{tr} \cup \{(\mathbf{x}, \mathbf{y}_{vic}, P_{\theta_{vic}}(\mathbf{y}_{vic}|\mathbf{x}))\};$
8: **end for**
9: // Train local model.
10: // Initialize the positive and negative datasets.
11: $\mathcal{D}_0^+ \leftarrow \mathcal{D}_q;$
12: **for** $(\mathbf{x}, \mathbf{y}_{vic}, P_{\theta_{vic}}(\mathbf{y}_{vic}|\mathbf{x})) \sim \mathcal{D}_{tr}$ **do**
13:    $\mathbf{y}_0^- \sim P_{\theta_t}(\cdot|\mathbf{x});$
14:    $\mathcal{D}_0^- \leftarrow \mathcal{D}_0^- \cup \{(\mathbf{x}, \mathbf{y}_0^-, P_{\theta_0}(\mathbf{y}_0^-|\mathbf{x}))\};$
15: **end for**
16: **while** $t < N_t$ **do**
17:    $t \leftarrow t + 1;$
18:    $\theta_t \leftarrow \theta_{t-1};$
19:    **for** $(\mathbf{x}, \mathbf{y}_{vic}, P_{\theta_{vic}}(\mathbf{y}_{vic}|\mathbf{x})) \sim \mathcal{D}_{tr}$ **do**
20:       $\mathbf{y}_t^+, \mathbf{y}_t^- \sim P_{\theta_t}(\cdot|\mathbf{x});$
21:       $\mathcal{D}_t^+ \leftarrow \mathcal{D}_t^+ \cup \{(\mathbf{x}, \mathbf{y}_t^+)\};$
22:       $\mathcal{D}_t^- \leftarrow \mathcal{D}_t^- \cup \{(\mathbf{x}, \mathbf{y}_t^-)\};$
23:    **end for**
24:    // Forward.
25:    **for** $\mathbf{x}, \mathbf{y}_{vic}, \mathbf{y}_{t-1}^+, \mathbf{y}_{t-1}^- \sim (\mathcal{D}_{tr}, \mathcal{D}_{t-1}^+, \mathcal{D}_{t-1}^-)$ **do**
26:       $\Delta^+ \leftarrow \log P_{\theta_t}(\mathbf{y}_{t-1}^+|x) - \log P_{\theta_{t-1}}(\mathbf{y}_{t-1}^+|x);$
27:       $\Delta^- \leftarrow \log P_{\theta_t}(\mathbf{y}_{t-1}^-|x) - \log P_{\theta_{t-1}}(\mathbf{y}_{t-1}^-|x);$
28:       **if** $\Delta^+ < \Delta^-$ **then**
29:          swap$(\mathbf{y}_{t-1}^+, \mathbf{y}_{t-1}^-);$
30:          swap$(\Delta^+, \Delta^-);$
31:       **end if**
32:       **if** $P_{\theta_t}(\mathbf{y}_{t-1}^+|x) < \tau_1$ && $\Delta^+ < \tau_2$ **then**
33:          $\mathbf{y}_{t-1}^+ \leftarrow \mathbf{y}_{vic};$
34:       **end if**
35:       // Compute loss with Equation 10 or 11.
36:       $\mathcal{L} \leftarrow \log[\frac{P_{\theta_t}(\mathbf{y}_{t-1}^-|\mathbf{x})}{P_{\theta_t}(\mathbf{y}_{t-1}^+|\mathbf{x})}] + clip(\log[\frac{P_{\theta_t}(\mathbf{y}_{t-1}^-|\mathbf{x})}{P_{\theta_t}(\mathbf{y}_{vic}|\mathbf{x})}]);$
37:       // Backward.
38:       $\theta_t \leftarrow \text{stepUpdate}(\theta_t, \mathcal{L});$
39:    **end for**
40: **end while**
41: **return** θ_t

MEA algorithms and theoretical analysis are still compatible with such conditions, we concede that concrete experimental validation and results beyond LaViSH settings are not presented here.

Lower-level Extractions. This study evaluates MEAs at the performance level, i.e., it measures the extraction effectiveness simply through task performance metrics, or the similarity of learned distributions to the victim model. This setting is justified, as performance metrics are essential for evaluating task-related knowledge and the practical application of LLMs. However, it does not consider the lower-level similarities between the victim and local models. Can we achieve neuron-level alignments in LLM's MEAs? How does a LaViSH setting hurt LLM's MEAs? Is it compatible to extract a MoE (Mix-of-the-Expert) Shazeer et al. (2017) victim model with a dense local model? These questions are not addressed in this research.